THE CORRELATION OF FORCE TO DEFORMATION OF THE MEDIAL ULNAR COLLATERAL LIGAMENT (MUCL) WITH CONSIDERATION OF BAND LAXITY

by

David Bernard Jordan

BSME, Louisiana State University, 2016

Submitted to the Graduate Faculty of

Swanson School of Engineering in partial fulfillment

of the requirements for the degree of

M.S. in Mechanical Engineering

University of Pittsburgh

2018

UNIVERSITY OF PITTSBURGH

SWANSON SCHOOL OF ENGINEERING

This thesis was presented

by

David B Jordan

It was defended on

August 15, 2018

and approved by

Patrick Smolinski, PhD, Associate Professor

William Slaughter, PhD, Associate Professor

Thesis Advisor: Mark Miller, PhD, Associate Professor

THE CORRELATION OF FORCE TO DEFORMATION OF THE MEDIAL ULNAR COLLATERAL LIGAMENT (MUCL) WITH CONSIDERATION OF BAND LAXITY

David B Jordan, M.S.

University of Pittsburgh, 2018

Overhand throwing performed at a competitive level generates extreme loading conditions at the elbow. The reaction loads that arise as a result of these conditions are supported by the biological structures within the elbow. One such structure is the medial ulnar collateral ligament (mUCL). In order to predict potential injuries, a thorough understanding of the ligament's response to such loads is required.

Previous works have shown the mUCL considered as two distinct portions, anterior and posterior, both of which possess different geometric and physical attributes [1]. In this study, the ligament is considered as being composed of three distinct portions. These are the anterior, middle and posterior bands. It is the combination of the responses of these bands that combine, through the principle of superposition, to form the response of the overall mUCL. In this work, the overall load-bearing response of the mUCL is determined by sequentially superposing each band as the laxity within each band is relieved upon loading. Determining the amount of laxity in each band provides the initial load-bearing length for the bands, necessary for strain calculation.

Seven cadaveric elbow specimens were used for the study. The intact mUCL of each specimen was tested under vertical distraction and then subsequently retested after two separate transections. The tests were performed within an MTS loading machine at four different flexion angles. The average slack in each band was found to be non-zero and flexion dependent. The

posterior and anterior bands were the most lax at full extension and full flexion, with an average slack of 2.7 mm and 2.2 mm respectively.

Individual band force-strain characteristics showed the anterior band to be the stiffest at the lesser flexion angles, with the middle band becoming the stiffest at the higher flexion angles. Overall mUCL force-strain profiles showed the ligament to be stiffest at 60° of flexion, with approximately 190N of force required for 2% elongation.

The presence of the laxity and the prominence of the mechanical responses of the individual bands, show the need for consideration of such factors when aiming to accurately portray the mechanical response of the mUCL.

TABLE OF CONTENTS

LIST OF TABLES

LIST OF FIGURES

1.0 INTRODUCTION

The elbow is important to the performance of daily living. The joint permits a large angular range of motion and transmits the forces between the upper arm and lower arm. These characteristic functions of the elbow allow people to perform their routine daily activities, as well as engage in more strenuous actions such as baseball pitching. Baseball pitching places great stress on the ligaments which hold the elbow joint together. The side of the elbow joint which faces toward the body is held together by the ulnar collateral ligament. This ligament complex is composed of three distinct ligaments, one of which, the anterior bundle (mUCL), has been identified as the primary support structure for the reactions that arise at the elbow when the forearm undergoes an outward angled moment. For everyday activities, this loading is small and rarely undertaken in a manner which can be harmful. However, this is a loading commonly required by baseball pitchers and generates large forces and torques at the elbow. The mUCL, consisting of multiple fibril bands, is subjected to these loading conditions during every pitch. As with any support structure, the mechanical response of the system, and all subsystems, to the imposition of loading conditions which commonly exist in the intended mode of application must be quantified. This will enable predictions to be made as to when the ligament may fail and who could be susceptible to injury.

1.1 MEDICAL TERMINOLOGY

The medical terminology relevant to the presented material will be defined. These terms include medial, lateral, distal, proximal, valgus, varus, anterior and posterior.

The terms medial and lateral pertain to the position of a particular body part relative to the midline of the body. This can be illustrated when discussing the elbow. In relation to the torso, the medial side of the elbow is the side closest to the torso. The lateral side of the elbow would then be defined as the opposite side, or outside of the elbow. The medial elbow is pictured in Figure (1).

The terms proximal and distal refer to the ends of an appendage in relation to the distance from the center of the chest. The proximal portion of an appendage refers to the end where it is joined to the body. The distal portion refers to the end furthest from the attachment point. In relation to this study, the ligament of concern would be located near the proximal ulna and the distal humerus, as pictured in Figure (2). The distal ulna would be near the wrist and the proximal humerus would be near the shoulder.

The terms valgus and varus are relevant to the concerns of baseball pitching and deal with the angulation. Valgus motion describes an outward angulation, while varus motion describes an inward angulation.

The terms anterior and posterior relate the front and back of a particular body part in relation to one another. The portion closest to the front is termed anterior. The portion closest to the back is termed posterior. For matters concerning this study, the anterior band of the mUCL is the segment of the ligament closest to the front of the elbow. The posterior band is the segment closest to the back of the elbow. The middle band of the ligament is defined as being directly in between the anterior and posterior. The alignment of these bands is shown in Figure (2).

1.2 ANATOMY

In medical terminology, the origin and insertion of a ligament refer to the beginning and end of the two ends, where the origin is the proximal end and the insertion is the distal end. The origin is often the more rigidly connected end and the insertion is the end which typically exhibits greater movement. The origin of the ulnar collateral ligament is at the base of the medial epicondyle, or the bottom of the humerus, and the insertion is at the ulna [2]. The medial elbow is depicted in Figure (1).

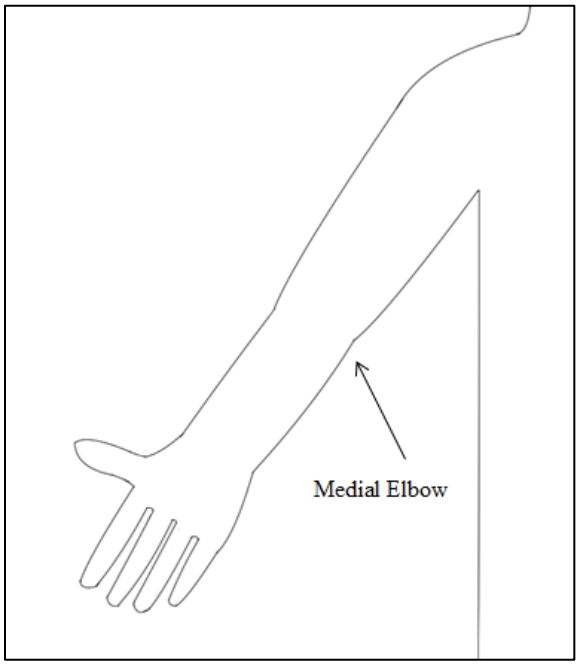

Figure 1. The Medial Elbow

The anterior bundle of the UCL (mUCL) originates at the medial epicondyle and inserts at the sublime tubercle at the medial coronoid process [3]. The mUCL consists of parallel collagen bundles [4], which have been commonly considered as two bands. These are the anterior and

posterior, respectively, and are located anteriorly and posteriorly with respect to the front of the elbow. The current work will consider the behavior of a third band, the middle band, which lies between the anterior and posterior bands. Figure (2) shows the medial elbow along with the UCL complex, mUCL and bone structure.

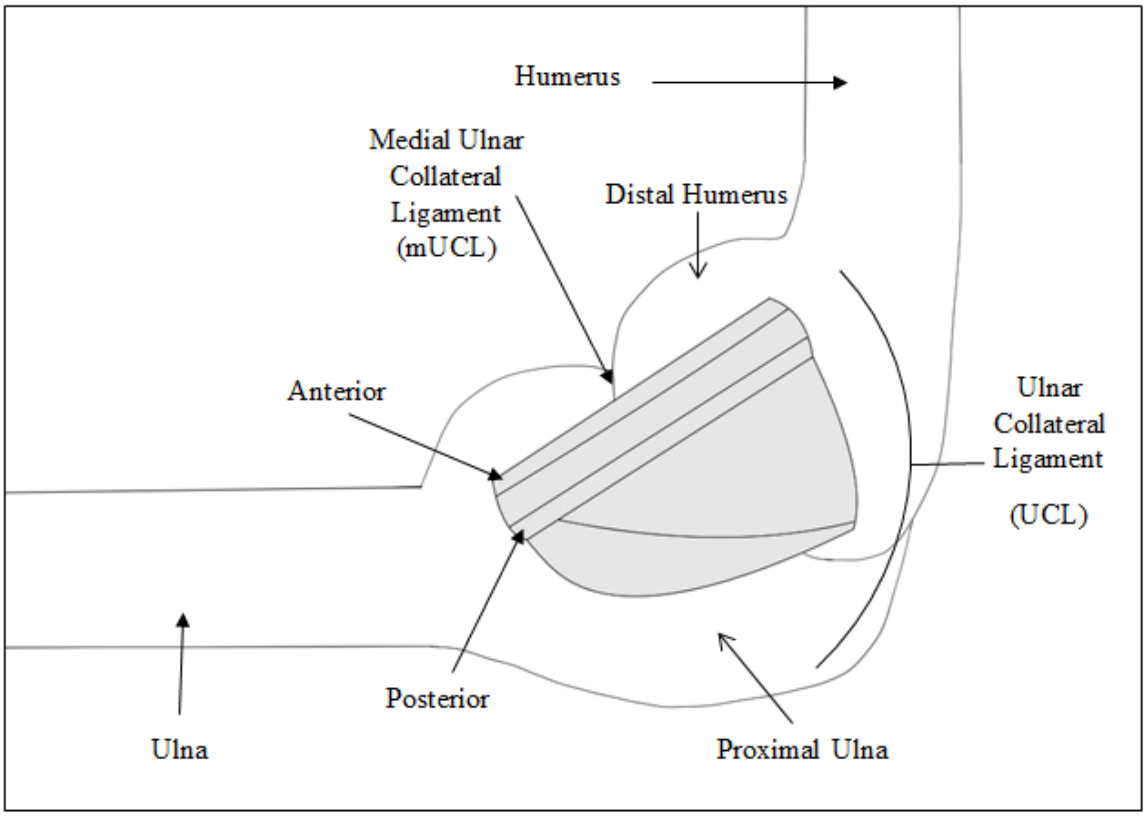

Figure 2. The Medial Ulnar Collateral Ligament

The geometry of the mUCL varies from person to person. One aspect of the geometry, the cross-sectional area, greatly affects the amount of stress that the ligament can withstand. This area is defined by the ligament width and thickness. The mean thickness of the ligament in the dominant elbow, 6.15 mm, is larger than that of the non-dominant elbow, 4.82 mm [5]. Proximally, the mean width is approximately equivalent to the width of the mid portion, 6.8 mm,

while the mean distal width of the ligament is slightly larger, 9.2mm [6]. The mean length of the ligament is 53.9 mm [7].

The variable width of the mUCL along its length is a testament to how unevenly stresses might distribute throughout the ligament. An uneven stress distribution highlights how each band of the ligament may be exposed to different forces. These anatomical observations further illustrate the need to quantify how much force each band will be subjected to supporting at any point throughout an incurrent deformation.

The relation of the force in each band to the deformation will depend on reliable measurements of strain. The idea of slack length will identify the portion of the ligament that remains tension-free during an imposed deformation, allowing for the identification of an appropriate reference length.

1.2.1 Research Question 1

In what sequence do the anterior, middle and posterior bands begin load support under the imposition of a linearly increasing force? Is there a slack length? Is there laxity in the native joint?

The working hypothesis is that a slack length does exist and at lesser flexion angles the anterior band will begin to support load first, while the posterior band will begin load support sooner at greater flexion angles.

1.2.2 Research Question 2

How much of the force carried by the overall mUCL is supported by the anterior, middle and posterior bands, individually, at different elbow flexion angles?

The working hypothesis is that at lesser flexion angles, the anterior band will support most of the load, with the roles of the middle and posterior bands increasing with increasing flexion angle.

1.2.3 Research Question 3

How do the behaviors of the individual bands affect the stiffness of the overall ligament?

The working hypothesis is that the stiffness of the overall ligament will be greatest at either of the intermediate testing angles, 30° or 60°. This is based on the observation that the ligament fibers tend to be less lax in the mid-section of the elbow flexion arc.

2.0 BACKGROUND

Many athletes perform overhand throwing motions across various sports. Throwing involves forceful rotations of the arm, causing the upper extremity to rapidly move through a quasi-circular arc and the associated linear and rotational kinematic quantities require substantial force and torque. This motion regularly exposes the athlete to dynamically extreme upper extremity loading.

These loads are transmitted through the shoulder, upper arm, elbow and forearm. Anatomically, these sites include intricate assemblies of ligaments and muscles. The evolutionary functionality of the ligaments in the upper extremity does not include the expectation of such repetitive high intensity loads and, therefore, the application of such loads inevitably causes damage.

A large number of reported injuries to baseball pitchers occur in the elbow [8], with a significant correlation of higher valgus elbow torque [9] and higher pitch velocity [10] with injury.

Identification of the mUCL as a critical ligament, in terms of supporting such loads and injury risk, is supported by three observations. These observations include the nature of the loading experienced by the elbow during a standard baseball pitching motion, the anatomical functionality of the mUCL and the reported mUCL clinical trends regarding baseball pitchers. Through analysis of the reported literature, a need for the analyzation of the mechanical nature of the mUCL will be evident.

2.1 BASEBALL PITCHING MECHANICS

There are six phases of the baseball pitching motion, each with its own respective mechanical influence on the upper extremity. These six phases have been identified [11]; the wind-up, stride, arm cocking, arm acceleration, arm deceleration and follow through. The kinematic variable associated with these phases is the elbow flexion angle (°); the dynamic variables are force (N) and torque (Nm).

Minimal variation in these variables is observed within the first two phases. Beginning with the arm cocking phase, the elbow is rotated backwards behind the head. As illustrated in Figure (3), this rotation produces a valgus torque, τ, at the elbow capable of reaching a maximum value of 64 – 120 Nm [11, 12] with a valgus loading rate of 29 Nm/s [13]. This torque is a reaction load necessary to prevent valgus deviation of the elbow. The range of the reported values suggests torque variation dependent on individual pitcher ability.

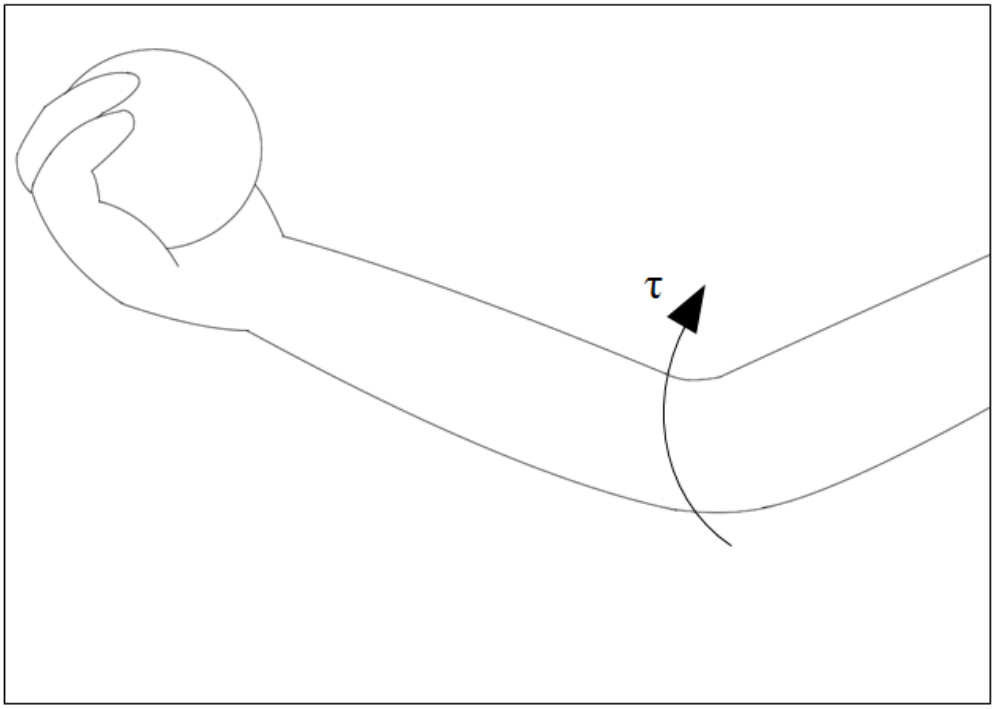

Figure 3. Valgus Reaction Torque at the Elbow during the Arm Cocking Phase

As the arm accelerates forward, several reaction forces are generated at the elbow. These include a medial, anterior and linear force. This linear force, shown in Figure (4), is a compressive reaction load responding to the application of the centrifugal force acting to distract the forearm out of the elbow joint [11], reaching a value of 150 N -390 N near the beginning of the arm acceleration phase [12].

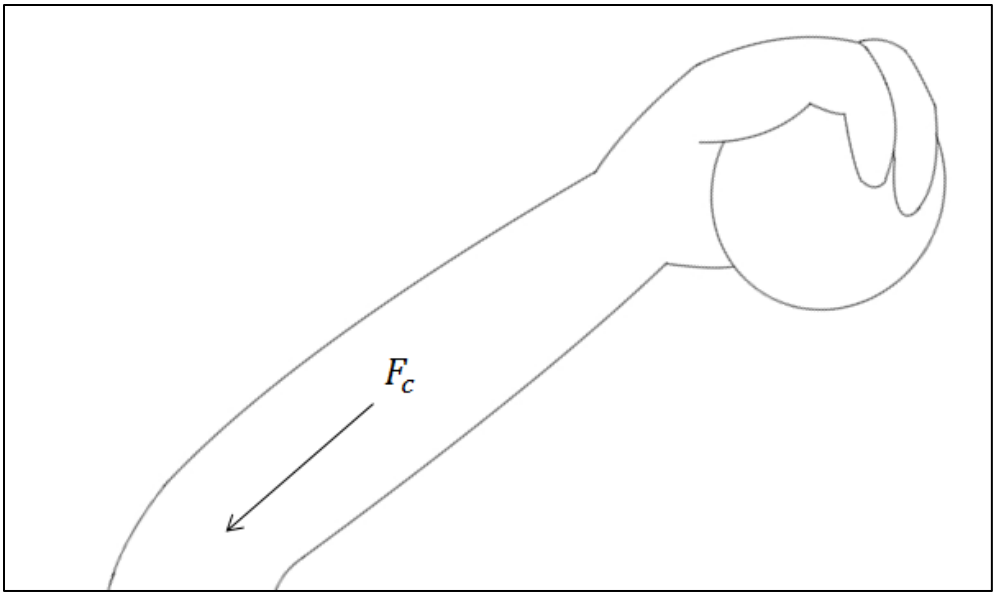

Figure 4. Compressive Reaction Load at the Elbow during the Arm Acceleration Phase

The time from the start of the arm cocking phase to the moment before ball release is signified by a sharp decrease in flexion angle. The angular change starts from the elbow flexion angle at maximum valgus torque and ends at the elbow flexion angle of ball release. During this motion, a maximum elbow extension velocity of 2300°/s has been calculated [11].

The magnitudes of these observed quantities illustrate the severity of the dynamic and kinematic effects that exist at the elbow during a baseball pitch. Further investigation will identify which of the elbow ligaments bear the majority of these influences.

2.2 MECHANICAL ANALYSIS

The geometric features of the mUCL such as length, width and thickness vary from person to person [14]. Because of this variation, a standard quantization of these geometric quantities is challenging.

The human elbow has a flexion angle range from 0° at full extension, to over 130° at full flexion. At full elbow extension, the fibers of the anterior band are taut, and the fibers of the posterior band are lax [2, 3]. This structural alignment at full extension leads to the appearance that the anterior band begins to support an imposed load more quickly than the posterior band.

As the flexion angle increases, the laxity of the posterior fibers gradually decreases and the anterior fibers remain noticeably taut up to approximately 85° of elbow flexion [1]. At flexion angles upwards of 90°, the posterior fibers are observed to be completely taut [2, 3], while the anterior fibers assume greater laxity. This reversal from full extension suggests that the expected load supporting sequence should likewise reverse, with the posterior band now expected to support an imposed load before the anterior band.

Valgus forces and torques of high magnitude are frequently exerted at the elbow of baseball pitchers. The role of stabilizing the elbow under such stresses is divided among the ulnar collateral ligament (UCL), anterior capsule, muscle and boney articulation, where the boney articulation refers to the joint surfaces between the humerus and ulna. At full extension, each of these articular and ligamentous components contributes equally towards valgus stress resistance, while the UCL provides most of the valgus stress resistance at higher flexion angles as it assumes the contribution of the anterior capsule [15]. Complete transection of the medial ulnar collateral ligament (mUCL), causes significant elbow laxity with application of a valgus force [16]. This observation identifies the mUCL as a primary contributor to valgus stabilization of the elbow.

The ability of the mUCL to effectively resist valgus stress depends on the distribution of these stresses among the posterior, middle and anterior bands. As previously noted, the anterior fibers remain taut while the posterior fibers gradually extend with increasing elbow flexion angle. Qualitatively, this suggests that the strains in the anterior band should remain relatively static and those of the posterior band should gradually increase, with respect to increasing flexion angle. This was quantitatively shown through digital tracking of elbows taken through a flexion arc between 40^{o} and 100^{o}, showing the role of the posterior band in valgus stability to increase with increasing flexion angle [17]. Transection of the anterior band and application of an external rotary moment showed significant increases in elbow laxity [18]. These studies identify the anterior band of the mUCL as a primary band for load support and elbow stabilization.

2.3 CLINICAL TRENDS

The mUCL has been identified as a primary supporter of elbow valgus stress, with the anterior band contributing primarily with respect to the middle and posterior bands. Being a primary ligamentous support structure, it is reasonable to expect the mUCL to be susceptible to injury. Upper extremity injuries account for 67% of pitcher injuries, with 25% occurring in the throwing elbow [8].

The mUCL has an ultimate failure load of approximately 260 N [1]. As observed in the mechanics of pitching, loads that exist at the elbow are of this magnitude or greater. Direct failure of the mUCL does not occur with every pitch because this tensile force is not directly applied to the ligament alone. The surrounding muscles of the elbow serve to alleviate most of the stress

[19]. Close to one hundred pitches are thrown every game, indicating that, while the mUCL does not experience the full brunt of this force at once, the ligament does experience a steady repetition of large forces. It is this repetition, with micro trauma, which leads to the failure of the mUCL [20].

The frequency of mUCL reconstructions among baseball pitchers has increased over the last forty years [21]. Reconstruction of the ligament is most commonly performed using a surgical graft whereby a different ligamentous structure, usually the palmaris longus tendon or gracilis tendon, is used to reconnect the medial epicondyle to the ulna [22]. These grafts may be passed through tunnels drilled through the distal humerus and proximal ulna, in a method known as the Jobe technique. A more modern method known as the docking technique utilizes similar methods with reduced drill hole size and simpler graft tensioning [23].

Mechanically, effectiveness of these grafts lies in their ability to restore the mechanical functionality of the elbow. Dynamically, the torsional stiffness of the reconstructed ligament is significantly less than that of the native ligament [24]. The native ligament also displays greater linear stiffness, exhibiting lower strain at maximal force, when compared to the Jobe and docking repair techniques [25], as well as lesser valgus laxity at lower flexion angles [26]. The observed decreases in torsional and linear stiffness, with respect to the native ligament, may result in greater mUCL deformation.

Athletically, reconstruction effectiveness can be evaluated by how quickly the athlete returns to competition and of the level of performance the athlete exhibits. On average, the return to pitching occurs approximately four months after reconstruction, with return to full competition after an additional eight months [27]. This year of absence from competition hinders the career advancement of the athlete.

Clinically, a successful reconstruction can be evaluated on the same athletic standards, with the additional consideration of surgical revision. Revision refers to a second UCL reconstruction. The rate of primary UCL revision reconstruction among professional baseball pitchers has been declining over the past forty years, with fifteen percent requiring one revision and one percent requiring two revisions [28].

2.4 MOTIVATION

Evaluation of the existing literature shows the mUCL to be an elbow ligament responsible for supporting baseball pitching and, consequently, susceptible to damage. Although most athletes who receive primary mUCL reconstruction are able to return to similar levels of competition, the mechanical properties of these reconstructions are often inferior to those of the native ligament.

With the extreme ligament loading conditions that baseball pitching creates, it is unlikely that these injuries can be completely eliminated, as shown by the increasing reconstruction rates. Therefore, an analysis of the mechanical properties of the mUCL and its bands can be used to advance preoperative conditioning techniques, improve early diagnosis of damage and possibly identify more compatible postoperative repair materials.

3.0 METHODOLOGY

Concept development for means with which to analyze the mechanical behavior of the mUCL and its three bands began with the fundamental knowledge base for ligamentous soft tissue force-strain behavior. When subjected to a tensile load, ligamentous soft tissue exhibit a mechanical response characterized by a piecewise force-strain curve [29]. The curve consists of two parts, an exponential and a straight line. The curve begins with the exponential and, after reaching a transition point, becomes linear.

The continuity of the piecewise model at this transition point was addressed by Kuxhaus et al [30]. The group recognized the deficiency of current models that did not impose the matching of the slopes at the exponential-to-linear transition point, and developed a Matlab (MathWorks, Natick, MA) code to do so. The code employs a five parameter model in conjunction with an optimization routine to develop the piecewise model for any set of empirically obtained force-strain data.

With the availability of this modeling tool, all that was needed was a reliable means of testing a specimen and obtaining the experimental data. Because the goal is to determine the mechanical response of three segments of the mUCL, all three segments need to be tested and represented by an individual set of response data. A standard approach to this problem involves transecting the ligament.

To divide the ligament into three segments and test each one individually would present several problems, as each segment would be very thin and hard to manually manipulate within a testing apparatus. Furthermore, in order to accurately represent the mechanical response of the

native ligament, it should remain in situ, in its natural anatomic station. This requires that the ligament should not be detached from its humeral origin and ulnar insertion.

Preserving the ligament in this state meant that the segments of the ligament had to be tested together. Although this eliminated the ability to directly develop individual response data for each segment, it did suggest a well-defined alternative option that could be used to infer the responses of the segments from the response of the total ligament. Through the use of superposition, a means to develop a force-strain response for different segments of the mUCL was available. The responses of these segments could then be assembled to construct the response of the total ligament.

A ligamentous structure could have an inherent amount of laxity which could cause a delay in the load-bearing response. This load-bearing delay, or slack length, represents the portion of the ligament which is supporting no load as the ligament is being strained. This length can be used to find an appropriate reference length for which to calculate the ligament strain.

With these considerations, an initial framework for accomplishing the goals of the proposed study was complete.

3.1 SPECIMEN PREPARATION

Seven cadaveric elbow specimens were prepared with the removal of all soft tissue surrounding the mUCL. The dissection resulted in the exposed ulna, humerus and mUCL.

The ulna and humerus were secured to the loading fixture using two PVC pipes, approximately 100 mm in length. The shaft of the humerus was placed into one pipe filled with polyester resin and allowed to harden. In order to preserve the natural alignment of the bone and

maintain the ulnar rotation axis parallel to the ground, the placing of the ulna into the PVC was done using an MTS (MTS Systems Corp., Eden Prairie, MN) machine. The humerus was secured within the MTS and the ulna was lowered into the PVC.

Once the ulna and humerus were secured, optical markers were placed along the length of the ligament. These are spherical markers approximately 0.8 mm in diameter and painted black. Markers were placed along the length of the ligament in three equally spaced columns, anterior to posterior, in order to most effectively delineate the three bands. Each row contained an equal number of markers, with one placed at the origin and insertion points on the humerus and ulna. Placing markers onto the bone of the humeral origin established a static reference position during the test and served as a datum for strain measurement.

Mounting the specimen in the fixture began with the insertion of the ulnar cylinder into the bottom fixture attachment. The machine was then aligned to bring the humeral cylinder into the top fixture attachment. Once inside the fixture, the ulnar cylinder could be moved in any cardinal direction in order to properly align the bones and minimize the space between the joint surfaces, while also maintaining proper alignment of the trochlea with respect to the coronoid process. The prepared specimen mounted into the loading fixture can be seen in Figure (5).

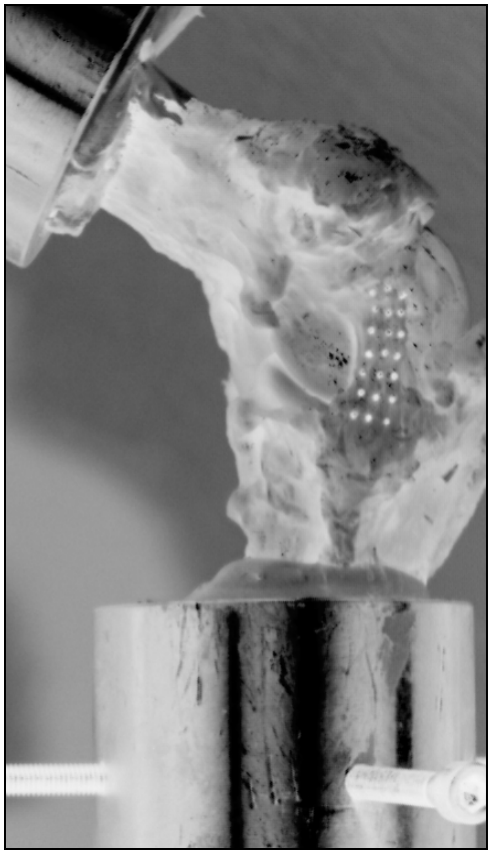

Figure 5. Prepared Specimen Mounted into Loading Fixture (reverse video)

3.2 LOADING FIXTURE

The loading fixture for the experiment is a custom design. There are three main features of the fixture. The first enables the inclusion of elbow flexion angle as an independent variable. The angle is controlled by a pin joint at the top of the fixture. This allows for the flexion of the specimen through a range of angles that vary from 0° to 105° in increments of 15°.

The second feature of the fixture allows the displacement controlled distraction of the mounted specimen. Distraction can be performed at different rates in a direction parallel to the vertical ulnar axis. This action subjects the specimen to loading scenarios that simulate the valgus

opening of the joint. The loads needed to achieve the imposed displacements are monitored in the output.

The third feature utilizes the rotational degrees of freedom that the load frame possesses. This feature enables the out-of-plane angle of the mounted specimen to be adjusted as needed in order to maintain proper joint capsule contact and alignment. With the ulna aligned along the distraction axis of the load frame, rotation of the humerus, by means of the load frame's axial rotation, accommodates the differences in anatomic alignment that may occur during mounting. The loading fixture is seen in Figure (6).

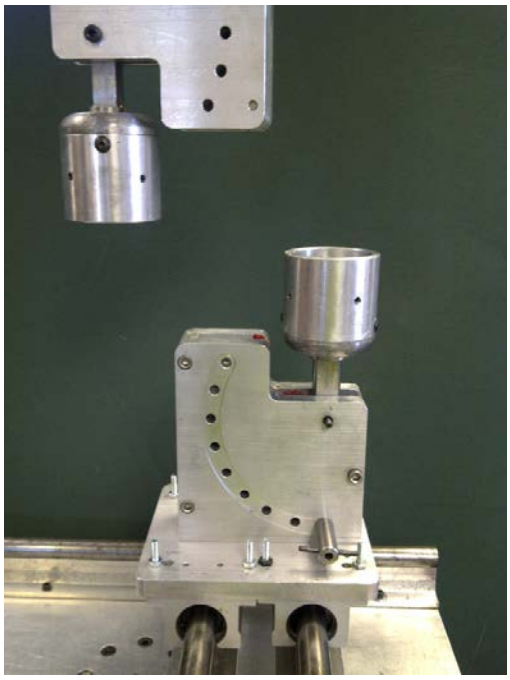

Figure 6. Loading Fixture

3.3 EXPERIMENTAL SETUP AND DATA ACQUISITION

Three pieces of equipment must be set up to perform the experiment; the loading equipment, the cameras, and the camera operation system. The first system was the loading fixture/ MTS, which consists of three components. The first was the loading fixture and crosshead assembly which was used to perform the physical test. The second was the computational and control system. This component was used to control the action of the MTS and was where all of the relevant data was recorded. The third was the analog to digital system (Measurement Computing, Middleborough, MA). Three analog to digital channels were used to store data on elapsed time, displacement and force.

The second system consisted of the cameras and camera mounts. In order to track the 3-D position of the optical markers, two Prosilica GC 1350C cameras (Allied Vision Technologies, Exton, PA) were used. These cameras were mounted onto a support structure and positioned for optimal viewing of the specimen. Calibration of the cameras utilized custom designed calibration frames with dimensions measured via coordinate measuring machine. The frame used for calibrating was placed in the spatial volume where the specimen would be tested. The cameras recorded the position of the frame and software quantified its relative dimensions, in 3-D, for comparison with those taken from the coordinate measuring machine. Error readings displayed the degree to which the cameras were able to accurately resolve the spatial position of the frame. The system is accurate to within 1% at 0.1 mm and 5% at 0.05 mm. The calibration process was complete once this error reached an acceptable minimum.

The third system was the camera operation equipment. The two cameras were plugged into a computer and their preparation and data logging was manually operated using Spicatech (Spica Technology Corp., Kihei, HI) vision software. Recording was automatically triggered once

the displacement began by a switch connected to the MTS control system. Upon distraction completion, all video recorded data was saved to the hard drive.

3.4 EXPERIMENTAL PROCEDURE

With the specimen secured in the fixture, testing began with the selection of the desired flexion angle. The top portion of the fixture, with the humerus, was locked with a pin into the desired angle. With the flexion angle selected, distraction was ready to commence.

The distraction was displacement controlled. A maximum vertical displacement was input and the resulting load was measured in the output. With a target value of 80N, the displacement would either be increased or decreased in order to achieve the target. This threshold was chosen because it is far less than the failure load, yet significant enough to produce appreciable strain. Three preconditioning cycles were performed; that is, three distraction cycles conducted in sequence, before the recording of the cycle to be analyzed. The preconditioning ensured that force-displacement relationship was repeatable. The recording was initiated during the pause after the final preconditioning cycle, with synchronization with the MTS analog to digital converter. Distraction was then repeated and the test performed for all angles (0°, 30°, 60° and 90°). The specimen, positioned at these angles, can be seen in Figure (7).

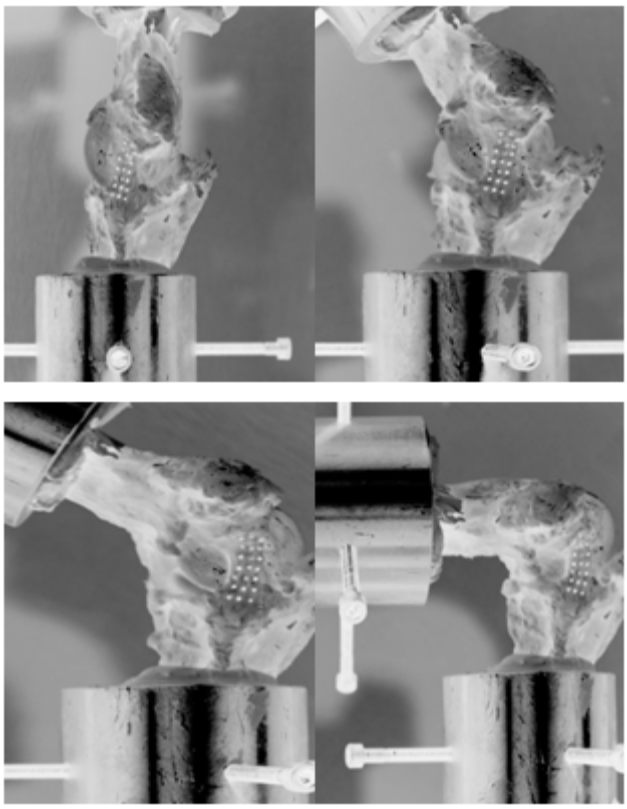

Figure 7. Specimen Elbow Flexion Arc (reverse video)

The dissection of the anterior band followed the test of the intact ligament. The specimen was carefully removed from the fixture and the anterior band was transected and removed. The specimen was then returned to the fixture and the entire testing procedure was repeated using the same displacements from the previous test. Upon completion of the second test, the specimen was again removed from the fixture and the middle band was transected and removed. The test was then repeated for the final time. Each stage of the transection cycle is shown in Figure (8).

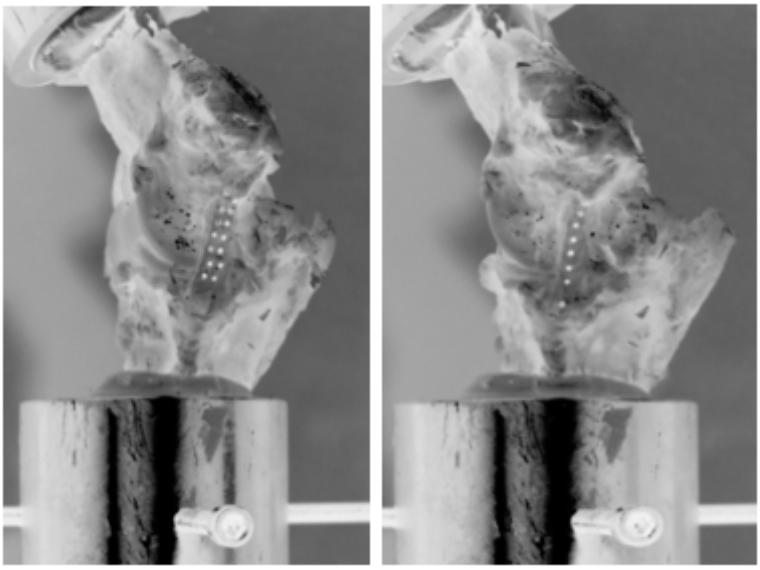

Figure 8. Ligament Transection Cycle. (Left) Anterior Band Transected (Right) Anterior and Middle Band Transected (reverse video)

3.5 STRAIN CALCULATIONS

The strain in the ligament was calculated in order to determine the longitudinal deformation that occurred in each band during each test. Engineering strains were calculated given by Equation (3-1).

$$\varepsilon = \frac{\Delta L}{L_o} \qquad 3\text{-}1$$

In this equation, ΔL was the change in the overall length of the band and L_o was the original length of the respective band. In order to track the 3-D movement of the markers, the film data was imported into the Spicatech motion tracking software. The motion of each marker was tracked

over the distraction period and a Microsoft Excel (Microsoft, Redmond, WA) file was exported containing the x, y and z coordinates of each marker. A sample representation of this data format for any particular marker is given in Table (1). The coordinates are output starting from the first frame of the video to the last, n^{th} frame. The distance formula, given by Equation (3-2), was used to calculate the distance between adjacent markers at each point in time. These distances are illustrated in Figure (9).

Table 1. Sample Marker Coordinate Data

Frame	X	Y	Z
1	x_1	y_1	z_1
2	x_2	y_2	z_2
n	x_n	y_n	z_n

$$d_i = \sqrt{(x_i - x_{i-1})^2 + (y_i - y_{i-1})^2 + (z_i - z_{i-1})^2} \qquad 3\text{-}2$$

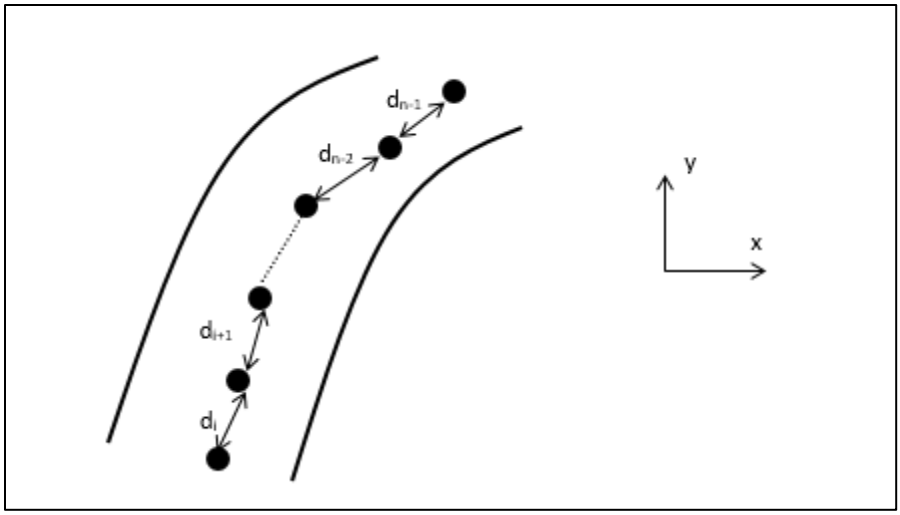

Figure 9. Distance Between Optical Markers along Ligament

With the distance between adjacent markers known, the overall length of the ligament at each moment in time could be calculated as the sum of the adjacent marker distances, using Equation (3-3).

$$L = \sum_{i=1}^{n-1} d_i \qquad 3\text{-}3$$

In this equation, n was the total number of dots along each band. This approach for calculating the band length was chosen in order to account for any curvature in the bands. With the length of the band known at every time increment, Equation (3-1) could be used to determine the strain at each time increment.

In Equation (3-1), ΔL was given by the difference between the length of the band at any specific point in time, L_i, and the initial length, L_o. The initial length was taken to be the length of the band at the point in time when the reaction load began to increase. These strains were calculated up until the time when the maximum load, i.e. maximum displacement, was reached.

This process was carried out for each ligament band of each test. This resulted in three sets of strain data for the intact ligament (posterior, middle, and anterior), two sets for the first transection (posterior and middle) and one set for the second transection (posterior).

Force and strain matrices were constructed for each test in order to keep account of the correct force-strain data pairs, with respect to time. A sample representation of these matrices is given in Tables (2), (3) and (4). These matrices were then imported into Matlab for further processing.

Table 2. Intact Ligament Force-Strain Matrix

Intact Ligament				
Time	Anterior Strain	Middle Strain	Posterior Strain	Force
t_1	ε_{a1}	ε_{m1}	ε_{p1}	f_1
t_2	ε_{a2}	ε_{m2}	ε_{p2}	f_2
t_n	ε_{an}	ε_{mn}	ε_{pn}	f_n

Table 3.Force-Strain Matrix for Ligament with Anterior Band Transected

Anterior Band Transected			
Time	Middle Strain	Posterior Strain	Force
t_1	ε_{m1}	ε_{p1}	f_1
t_2	ε_{m2}	ε_{p2}	f_2
t_n	ε_{mn}	ε_{pn}	f_n

Table 4.Force-Strain Matrix for Ligament with Anterior and Middle Band Transected

Anterior and Middle Band Transected		
Time	Posterior Strain	Force
t_1	ε_{p1}	f_1
t_2	ε_{p2}	f_2
t_n	ε_{pn}	f_n

3.6 SUPERPOSITION PRINCIPLE

The principle of superposition states that the overall reaction of an entity subjected to multiple stimuli can be determined by separately considering the effects of the individual stimuli and combining the results. This principle holds for small elastic deformations and if the stimulus and reaction are linear. In this study the stimulus is the displacement and the reaction is the load. Each ligament band represents an individualized system whose added effects contribute to the total system of the intact ligament.

To justify the use of the principle, it was necessary to check the conditions of the two requirements. The linearity condition was satisfied if the independent variable of the experiment, displacement, and the dependent variable, force, were both linear. Figure (10) shows the displacement vs time graph for the intact mUCL of a particular specimen at 90° of flexion. Figure (11) shows the force vs time graph for the same specimen.

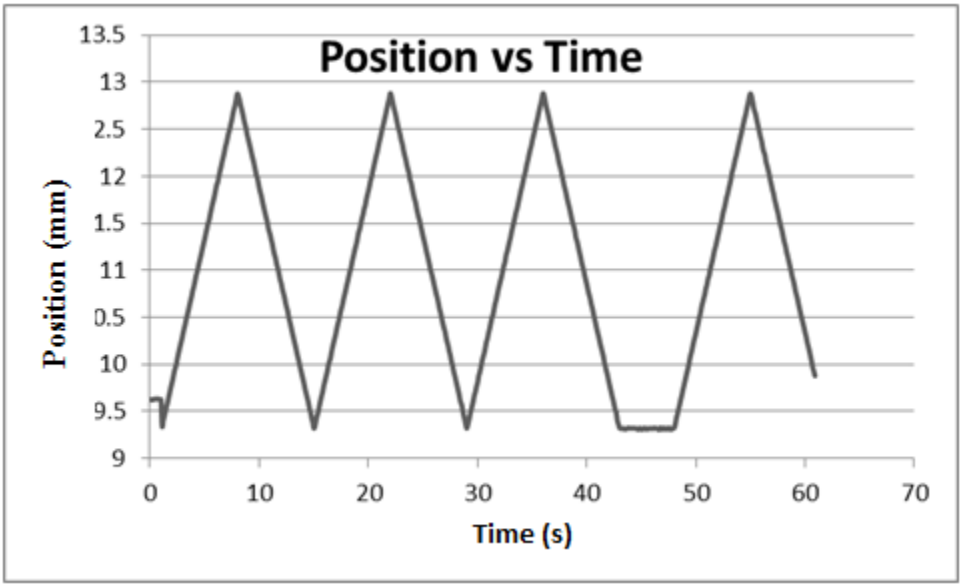

Figure 10. Position vs Time for Intact mUCL

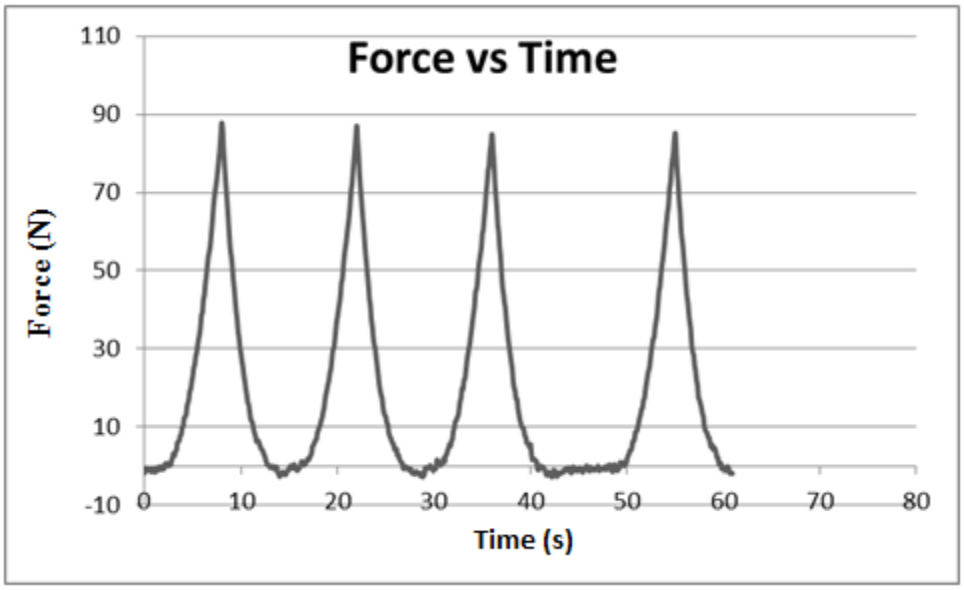

Figure 11. Force vs Time for Intact mUCL

Figure (10) showed the independent variable, displacement, to be completely linear. This showed that the linearity requirement for the stimulus was satisfied. However, Figure (11) showed the dependent variable, force, to be only partially linear. This was expected because soft tissues display a piecewise force-strain response. This can be seen in Figure (11) as the response gradually transitioned from an exponential nature to a linear one.

Taking this inherent feature of soft tissues into account, it was clear that the linearity condition for superposition could not be completely satisfied. However, when observing the response, it was evident that the linear region dominated the majority of the behavior. The duration of the exponential region was relatively small and the force values within this region were insignificant in comparison to their linear counterparts. With these observations, it was assumed that the linearity conditions for superposition were sufficiently satisfied due to the tendency of the

linear behavior to significantly out-weigh the exponential behavior in regard to duration and force magnitude.

In order to complete the justification for using the superposition principle, it was necessary to show that the deformations experienced by the tested specimen were sufficiently small. No current standard existed for what class of deformations was to be considered sufficiently small, so a mechanical sense of the definition was utilized. For this study, deformations were considered to be sufficiently small if the loads needed to produce such deformations were substantially less than the failure load of the ligament. This ensured that the material retained its elastic properties and that further tests could proceed with confidence that the resulting data remained uninfluenced by any plastic deformational effects.

As seen in Figure (11), the maximum load achieved for this particular specimen was approximately 90N for an approximate displacement of 3.5 mm. This maximum load reached at the peak displacement was much less than the 260N failure load of the ligament. With maximum loads of this magnitude, it could be assumed that no permanent damage was caused to the ligament and the condition for small entity deformation was satisfied.

3.7 MATLAB PROCESSING

In order to determine the force-strain behavior of the individual bands and that of the entire ligament, a custom Matlab code was created. The code incorporated the force-stain behavior of each band with any slack length that each possessed, in order to form the force-strain characteristic for the overall mUCL. To illustrate the output of the code, each step is explained in detail followed

by the result. These outputs were from the results obtained from a particular specimen at 90° of elbow flexion.

The code was comprised of eight functions. These functions operated in sequence, producing output variables which were used as inputs for the subsequent function. These eight functions could be categorized into two groups based on their respective actions. Group one was the exponential-to-linear model approximation group. The functions of this group output the piecewise model parameters for each band. Group two was the empirical-to-modeled error minimization group. The functions of this group output the error which existed between the empirical and modeled data. The parameters of group one were determined through a minimization routine aimed at reducing this error. Both of these functions were from the work of Kuxhaus et al [30].

3.7.1 Band Slack Length

The first function of the Matlab sequence determines the slack length in each band, where slack length is defined as the extra length that a ligament band must elongate through before it begins to carry load. The goal of this process is to determine a strain offset for each band. This strain offset represents the strain value of the intact ligament where the band becomes taut and starts to contribute to load bearing.

The problem was considered as three springs oriented in parallel. The springs have different stiffness values and different slack lengths. Because of this, under the influence of an applied load, each spring will start to contribute to load support at different times and support different amounts of load. With no slack lengths, the stiffer spring will begin to load first. Through superposition, each spring is treated as an individual entity, uninfluenced by the others. Therefore,

the amount of displacement each spring experiences is determined solely by its respective material/structural properties.

Once the leading spring is strained to a certain amount, the second stiffest spring will begin to bear load. Because the second spring is now contributing to load support, the overall construct stiffness increases. The overall reaction of the construct is now equal to the combined reaction of both springs.

As the load continues to increase, the leading and second springs continue to strain until they reach a certain value of strain whereby the final spring begins to bear load. With the third spring now contributing to load support, the construct grows even stiffer and has a reaction equal to the combined reaction of the three springs.

The leading spring represents the respective ligament band which begins to strain first. As the strain measures the overall displacement of the ligament, it is the strain of the leading band which represents the overall strain of the ligament. The strain of this leading band, at the time when the second band begins to bear load is the overall ligament offset strain for the second band. Likewise, the strain of this leading band, at the time when the third band begins to bear load is the overall ligament offset strain for the third band.

The observation that each band registered no load before the band was taut allowed for the identification of the time interval over which the slack was removed from the band. It was the time interval on the strain vs time plot over which the strain remained approximately zero. At the end of this time interval, when the strain vs time curve first began to increase, was the time when that respective band began to bear load.

The strain vs time plot for each band of the intact ligament is shown in Figure (12). The indicators on the time axis designate the respective point in time where each band began to incur

strain. An algorithm within Matlab was used to approximate this point. The basis of the method was analogous to finding the first point on the curve where the derivative became positive. The difference between the maximum recorded strain value and each recorded strain was taken and recorded in a separate vector. The value within this vector whose difference was closest to the maximum strain value was selected as the point of initial strain increase.

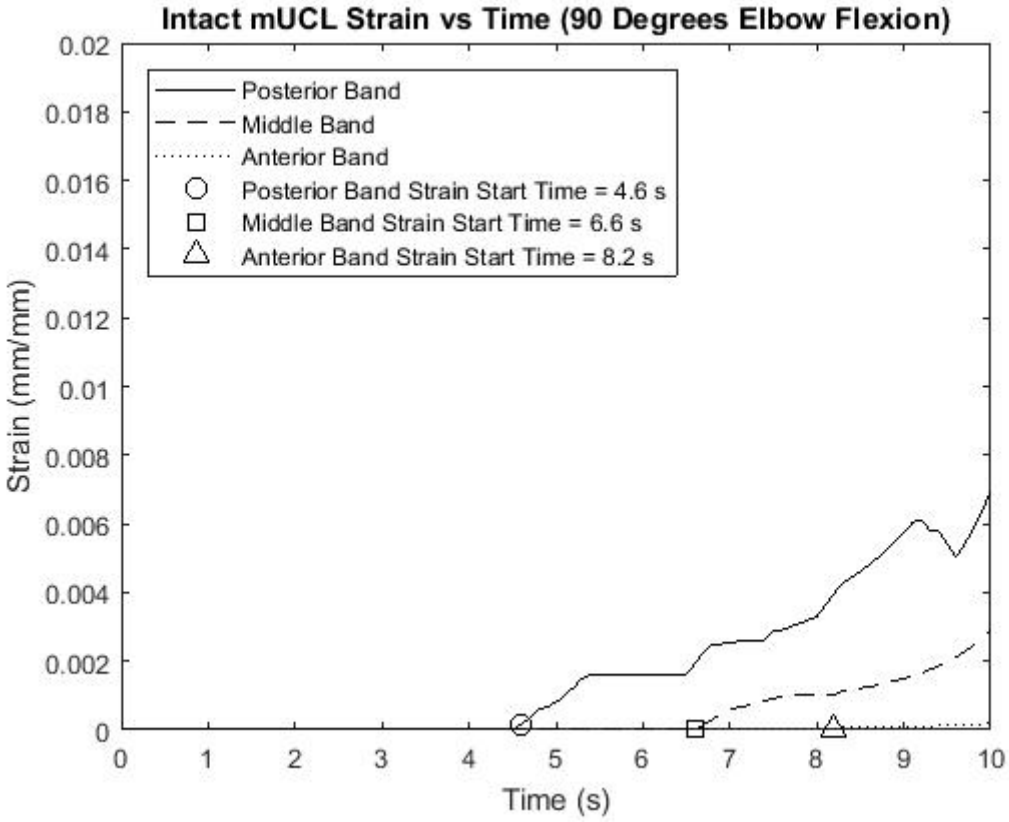

Figure 12. Strain vs Time Plot for Each Ligament Band

The band which began to increase in strain first was taken as the leading band with an overall ligament offset strain of zero. The offset strains for the second and third bands were determined by taking the time at which their respective strain started to increase and finding the

strain of the leading band at that time. These offset strains for the represented specimen are shown in Figure (13).

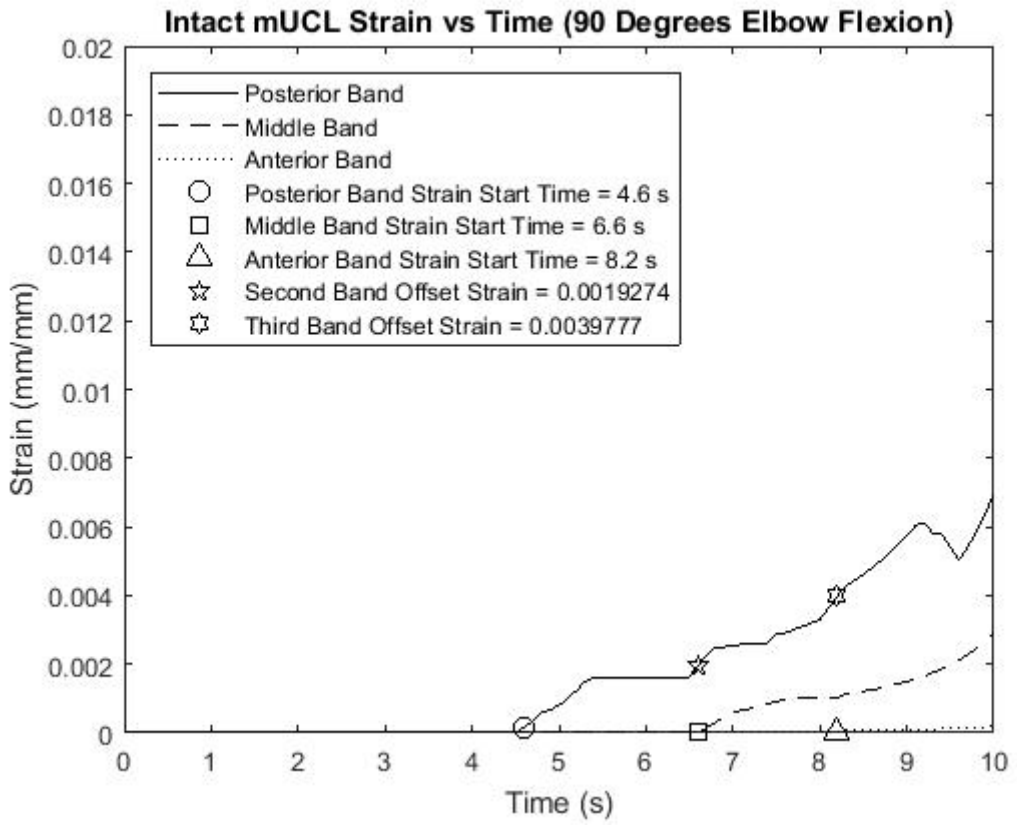

Figure 13. Offset Strains for the Second and Third Bands

3.7.2 Posterior Band Model Parameters

After finding the slack lengths, the Matlab program determined the model parameters for the posterior band. The process started with the force and strain data collected from the final test performed on the ligament with just the posterior band intact. The dots of Figure (14) represented the empirical force-strain data for the posterior band. The strains were taken over the interval of

time starting at the time of initial strain increase and ending at the time of maximum load. The curve of Figure (14) shows the data fitted to an exponential-linear piecewise model, represented by Equation (3-4). The star represents the coordinate of the strain value, ε_p, and the force value, F_p, where the graph transitions from exponential to linear behavior. The parameters for the model (a, b, c, ε_p, and F_p) were determined through a minimization routine (fmincon). A separate, error, function was defined which produced the difference between the empirical and modeled forces. The minimization routine was configured to find the parameters of the exponential to linear model which minimized the output of this error function.

$$F = a(e^{\varepsilon b} - 1) \qquad \forall \varepsilon < \varepsilon_p$$
$$F = c(\varepsilon - \varepsilon_p) + F_p \qquad \forall \varepsilon \geq \varepsilon_p \qquad \text{3-4}$$

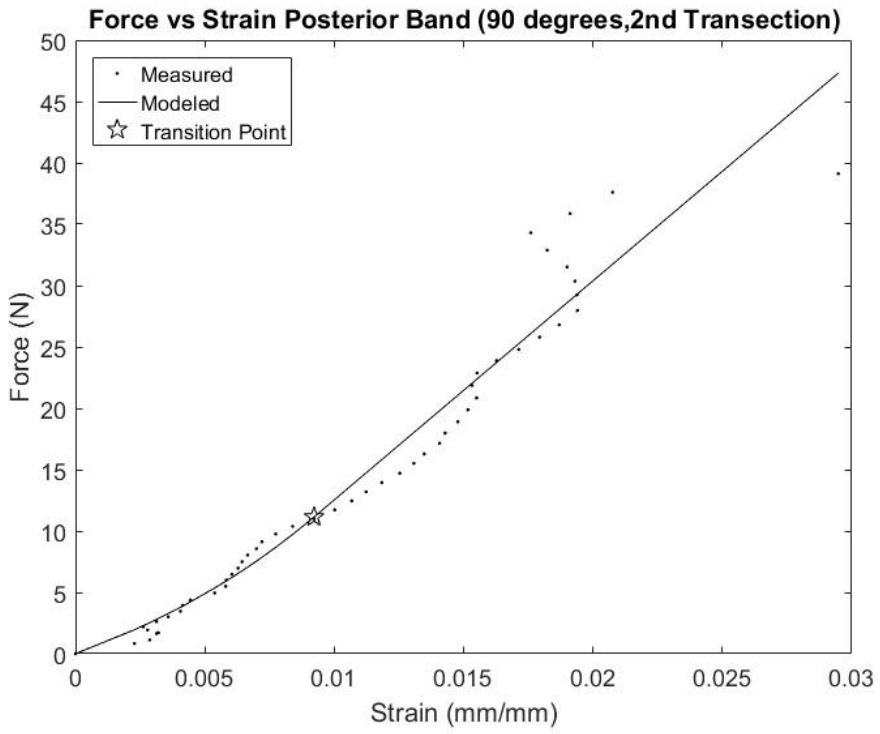

Figure 14. Force vs Strain for the Posterior Band

The core of the remaining program lied within this initial step. Because the posterior band was the only band present during the test of the second transection, its behavior was completely uninfluenced by the other bands. This guaranteed that the registered force and strain values only involved the posterior band. Therefore, this experimental data and the resulting model are presumed to completely represent the behavior of the posterior band.

Through superposition, the posterior band was viewed as an individualized entity and maintained its own characteristic behavior as a part of the ligament, whether the other two bands were present or not. This behavior was held constant throughout the remainder of the program.

3.7.3 Middle Band Model Parameters

The program then took in the model parameters for the posterior band as inputs and determined the model parameters for the middle band. The empirical data of force and strain were input from the first transection test performed on the ligament with only the posterior and middle bands intact. These forces were known to be distributed, in some unknown proportion, between the posterior and middle band.

At any one instant in time, the total load carried and the strain in each band was known through measurement. The behavior of the posterior band was completely known, thus, the load carried by the posterior band at any value of posterior band strain was known. The total load carried by the middle band was thus given by Equation (3-5). It was equivalent to the time-specific difference between the total force measured and the load carried by the posterior band at that time-specific empirical posterior band strain value.

$$F_{middle_i} = F_{total_i} - F_{posterior_i} \qquad 3\text{-}5$$

This calculation provided a vector of forces present in the middle band. In order to obtain the modeled strains, a reverse application of the exponential-to-linear piecewise model was used. Represented by Equation (3-6), the calculated forces were used as inputs to determine the resulting strains.

$$\begin{aligned} \varepsilon &= \ln\left(\frac{F}{a} + 1\right) b^{-1} && \forall F < F_p \\ \varepsilon &= (F - F_p)c^{-1} + \varepsilon_p && \forall F \geq F_p \end{aligned} \qquad 3\text{-}6$$

Unlike the previous minimization routines that analyzed the error between the empirical and modeled force values, the subsequent minimization efforts involved the error between the empirical and modeled strain values. The empirical strain values were those strains measured for the middle band during the first transection test and the modeled strains were those produced by Equation (6). The middle band parameters were then produced subject to minimizing this error.

3.7.4 Anterior Band Model Parameters

After determination of the middle band parameters, the program then used the model parameters for the posterior and middle bands to determine the model parameters for the anterior band. This process began with the extraction of the force and strain data from the test performed on the ligament with all three bands intact. These forces represented the total force born by the intact ligament and were distributed in an unknown fashion throughout the three bands.

From the previous calculations, the forces present in the posterior and middle bands at any strain value were known. Through superposition, the force in the anterior band at any instant in time was equivalent to the difference between the total force measured and the sum of the forces present in the posterior and middle bands at that same time. This is represented by Equation (3-7).

$$F_{anterior_i} = F_{total_i} - F_{posterior_i} - F_{middle_i} \quad 3\text{-}7$$

With the anterior forces determined, a similar analysis as that performed for the middle band, using the inverse exponential-to-linear model, was utilized to determine the appropriate anterior band strain values. Figure (15) shows the modeled force-strain loading behavior for all three bands of the represented specimen.

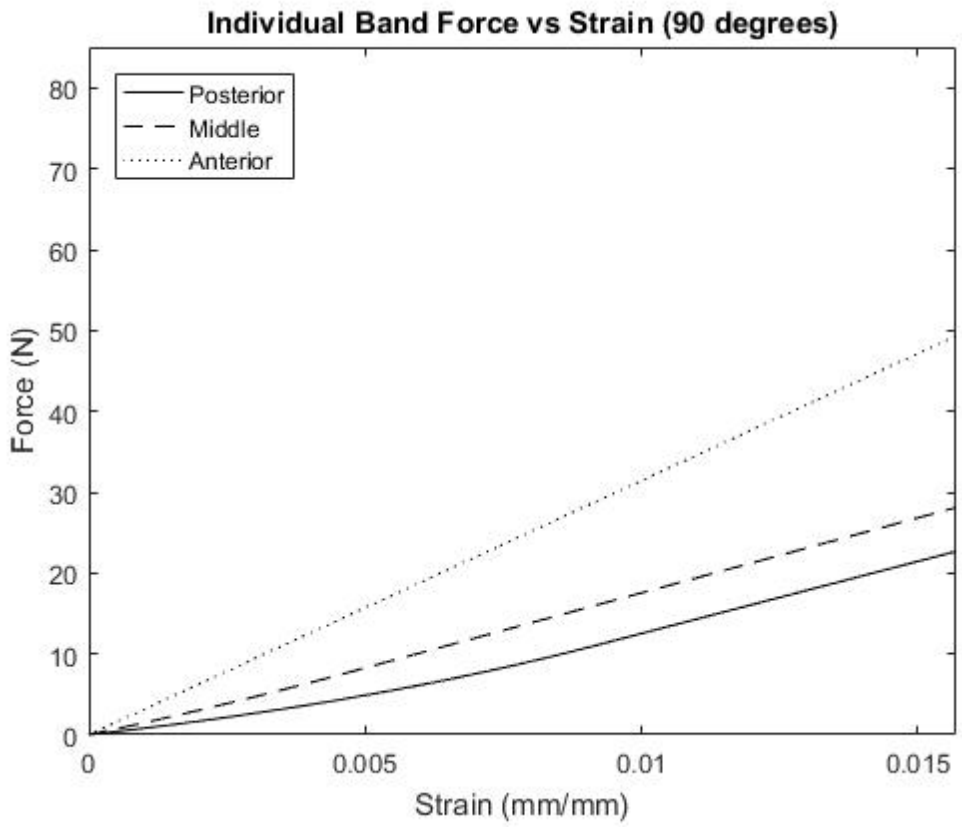

Figure 15. Force vs Strain for all Three Bands

3.7.5 Overall mUCL Model Parameters

With the individual force-strain behavior determined for all three bands of the mUCL, the next step was to determine the force-strain behavior for the overall ligament. The last step in the program determined the model parameters for the overall mUCL using the model parameters for the posterior, middle and anterior bands.

In reference to the model of the three parallel springs, the general shape of the overall ligament force-strain curve could be inferred. Before developing the Matlab routine to conduct the analysis, a general expectation was developed with which the outcome could be compared. In

consideration of slack length, the force-strain curve should start at a strain of zero and, with increasing load, start to increase in strain with the behavior of the leading band.

Once the offset strain value for the second band is reached, the nature of the curve becomes that of the combined behaviors of the two bands. This should cause the slope of the curve to increase beyond the point of the first offset strain value, characterizing an increase in stiffness. Once the offset strain value for the third band is reached, the response becomes that of all three bands combined. This should cause an even greater increase in slope in the portion of the graph beyond the second offset strain value, characterizing the stiffness increase from the inclusion of the third band.

The resulting shape is expected to be piecewise but continuous, consisting of one force-strain curve that is the combination of three separate curves. Because the curve is expected to be piecewise, the existence of any discontinuous points must be considered. Any discontinuous points that may exist would likely appear at the two offset strain values. This observation was based on the fact that the model could experience an instantaneous increase in force resulting from the inclusion of the additional band. This increase in force is reasonable because the ligament is expected to get stiffer as the bands sequentially lengthen, thus resulting in greater forces needed to continue deformation.

To ensure that no discontinuities existed within the model, the program imposed a continuity condition at the two offset strain values. Once the first offset strain value was reached, the leading band was strained to a value of force known from its individual force-strain model. The second band, which had just eliminated its slack, was now fully taut but still had a strain value of zero. This required that the force in this band also be zero. This condition imposed that the sum of the forces from the two bands be equivalent to only the force in the first band. This

mandated that the value of force observed at each offset strain value was equal from either left or right approach, thus, ensuring continuity. Figure (16) shows the resulting force-strain profile for the overall ligament and the approximate overall ligament strain values at which each band began to bear load.

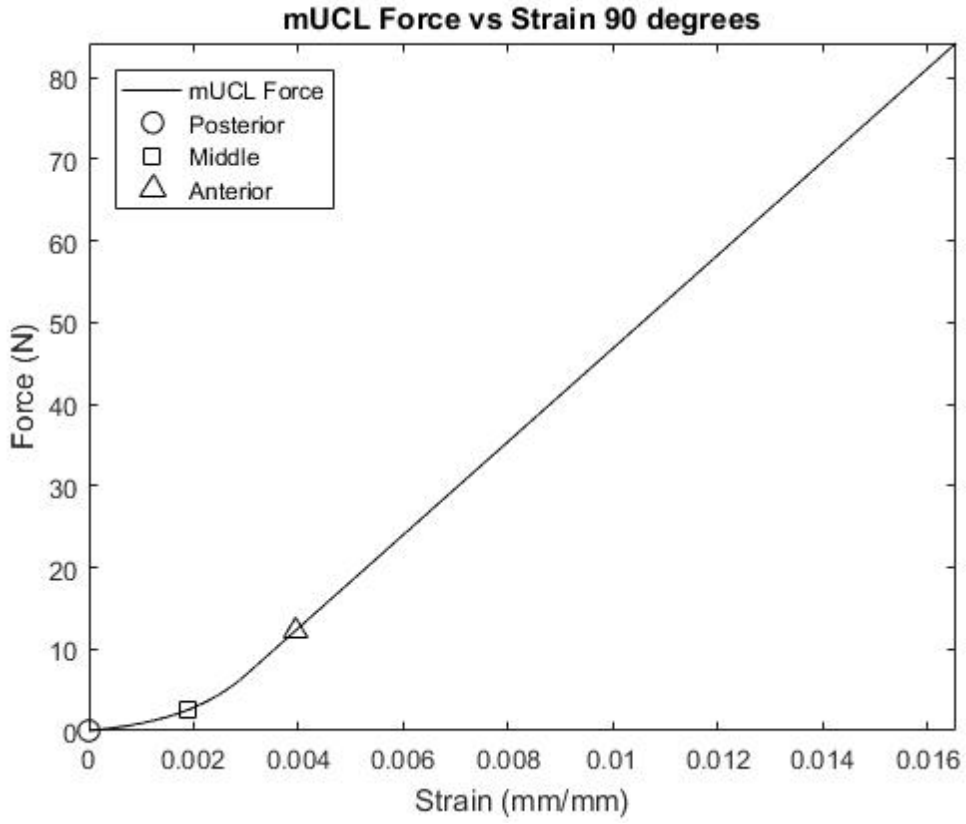

Figure 16. Force vs Strain for Overall mUCL

The maximum force value carried by the overall ligament was equal to the maximum force registered from the test performed on the intact ligament. Based on the principle of superposition, this was an expected result. The sum of the forces carried by each individual band should be equivalent to that carried by the whole ligament.

4.0 RESULTS

4.1 SLACK LENGTH

The offset strains for each band varied between specimen and across each flexion angle. A mean value of offset strain was calculated for each band at each angle in order to analyze how the bands were tending to sequence in regards to load-bearing. At each angle, the band which displayed the least amount of offset strain was termed the leading band. The offset strains for the second and third bands represented the amount of strain that the leading band had at the point in time when the second and third bands began to bear load. These offset strain results, averaged over the seven specimens, are shown in Figure (17).

The slack length results represented the amount of slack each band had to elongate through before they were able to incur strain. These results were obtained by multiplying the distraction rate by the elapsed time over which the strain for each band remained zero on the strain-time plot. The results for the seven specimens were averaged together and can be seen in Figure (18).

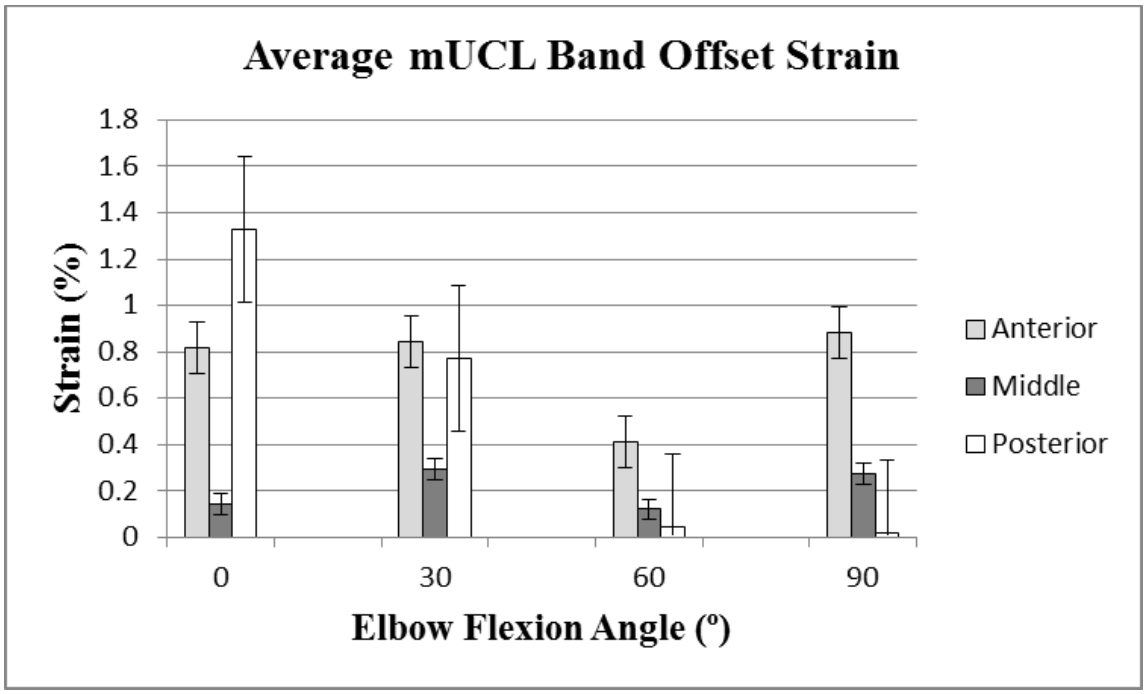

Figure 17. Average mUCL Offset Strain Results for Each Band

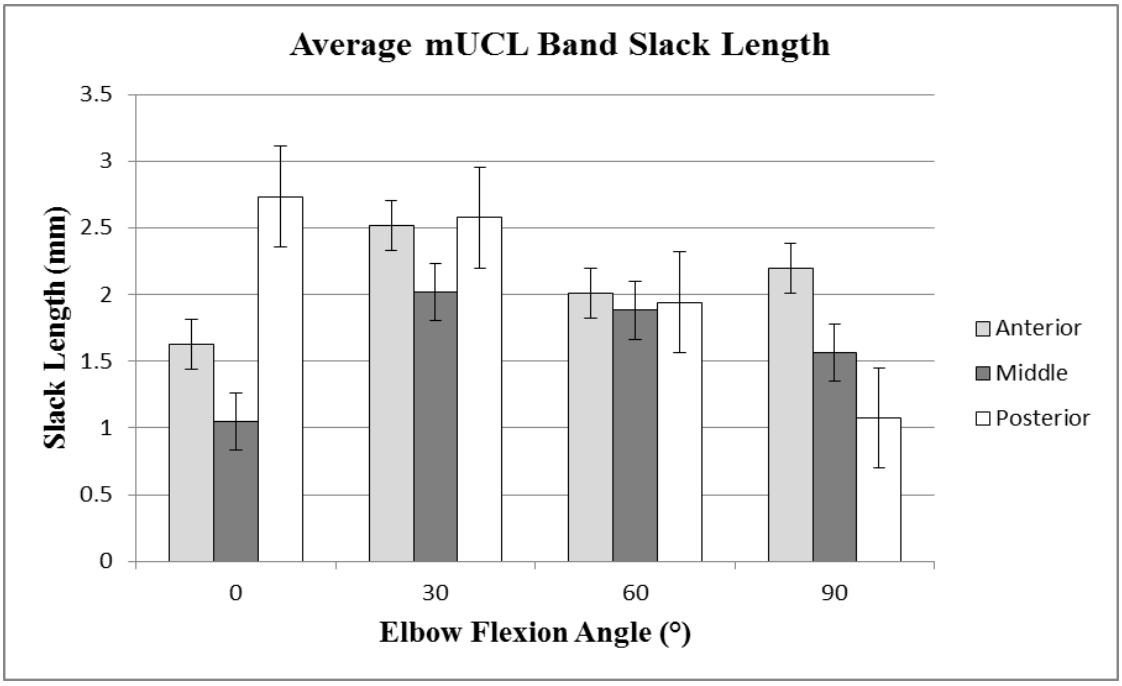

Figure 18. Average mUCL Band Slack Length

At 0° and 30° of elbow flexion, the anterior band had the second greatest slack amongst the three bands. At 60° and 90° the anterior band had the greatest slack. On average, the middle band had the least slack at 0°, 30° and 60°. At 90°, the middle band had the second greatest slack amongst the three bands. The slack of the posterior band was observed to steadily decrease from 0° to 90°, having the most amongst the three bands at 0° and the least amongst the three bands at 90°.

4.2 STIFFNESS

Using the force-strain curves for the individual bands, the stiffness of each band could be determined. Because the force-strain curves were piecewise in nature, the prescribed strains needed to be representative of the regions on both sides of the exponential/linear transition point, as well as be within the range of the experimentally achieved values. For this reason, strains of 0.5%, 1% and 2% were chosen. At each angle, the force born by each band at each of these specified strains was calculated from each of their respective force-strain profiles and averaged together over the seven specimens. The results are shown in Figures (19), (20) and (21).

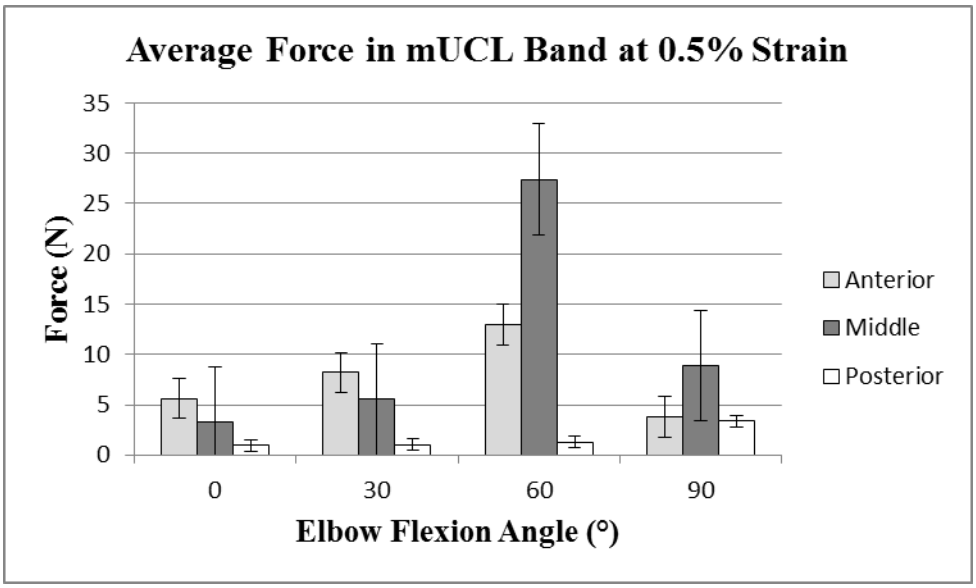

Figure 19. Average mUCL Band Force at 0.5% Strain

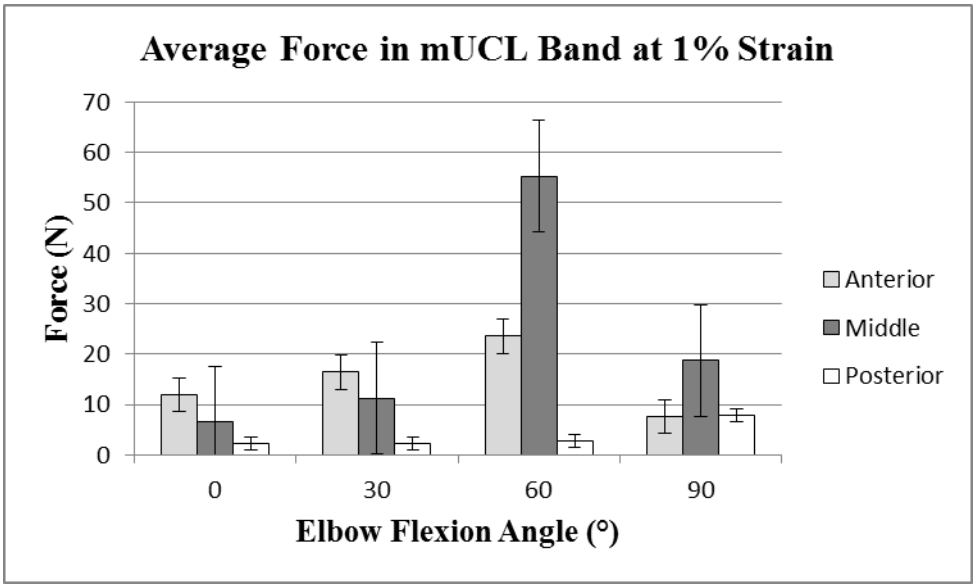

Figure 20. Average mUCL Band Force at 1% Strain

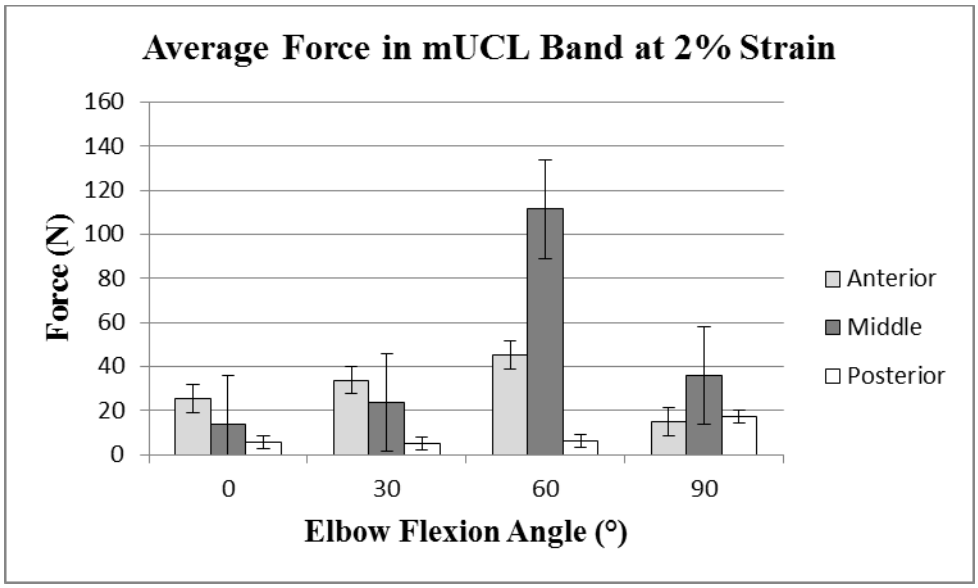

Figure 21. Average mUCL Band Force at 2% Strain

On average, the anterior band had the greatest stiffness at 0° and 30° of elbow flexion. The middle band had the greatest stiffness at 60° and 90° of flexion. The posterior band was the least stiff of the three bands at the flexion angles of 0°, 30° and 60°.

4.3 OVERALL LIGAMENT STIFFNESS

The results for the total ligament stiffness are presented in Figure (22). Prescribed values of strain were held constant and the resulting forces, calculated from the total ligament force-strain models, were extracted for each angle and averaged together over the seven specimens. This was done for strain values of 0.5%, 1% and 2%.

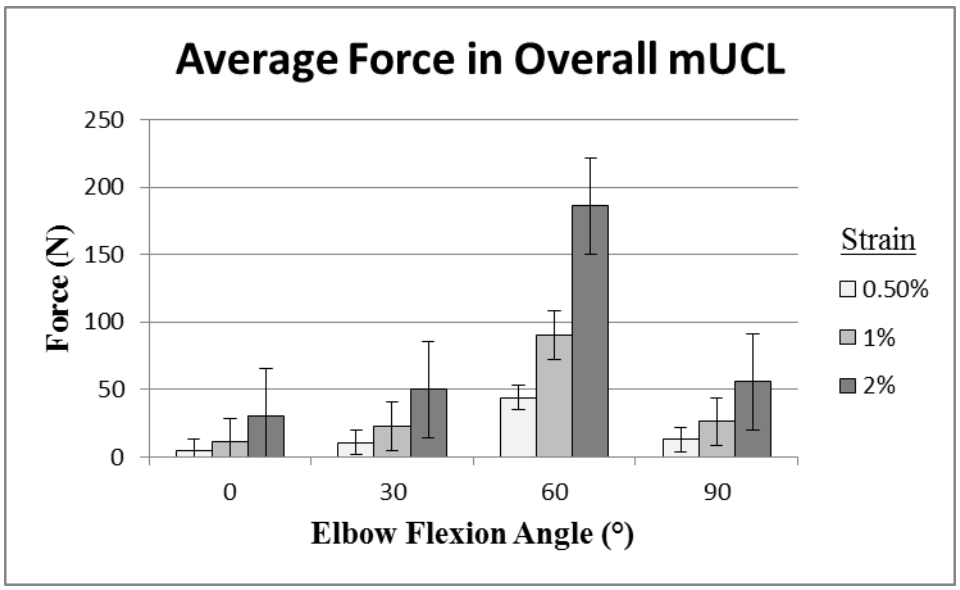

Figure 22. mUCL Force at 0.5%, 1% and 2% Strain

On average, the stiffness of the overall mUCL increased from 0° to 30° of elbow flexion and from 30° to 60°. The mUCL experienced a decrease in stiffness from 60° to 90°. The ligament had the greatest amount of stiffness at the elbow flexion angle of 60°.

5.0 DISCUSSION

5.1 SLACK LENGTH

At 0° and 30° of elbow flexion, the anterior band had the second most slack amongst the three bands. This does not support the observations during the experiment which appeared to show the anterior portion of the ligament to be relatively taut at the lesser flexion angles. At 60° and 90° the anterior band had the greatest amount of average slack. This suggested that the anterior band tended to begin load-bearing last at these angles. This supported qualitative observations showing the increase in laxity of the anterior fibers as the elbow was flexed.

On average, the middle band had the least amount of slack at 0°, 30° and 60° of elbow flexion, suggesting that the middle band began load-bearing first at these angles. At 90°, the middle band had the second greatest average slack amongst the three bands.

Previous works delineated the mUCL into the anterior and posterior bands only. The added demarcation of the middle band was bound to contain some posterior and anterior fibers. This could explain why at 0°, 30° and 60°, where the anterior band was expected to have the most slack, the middle band displayed the behavior expected of the anterior band. This could also explain why at 90°, where the amount of greatest slack shifted from the anterior band to the posterior band, the middle band exhibited a behavior directly intermediate of the two.

The average slack of the posterior band steadily decreased from 0° to 90°. Observation of the posterior fibers could explain this result. These fibers had the greatest amount of laxity at full extension, resulting in the posterior band's highest value of slack existing at 0°. As the elbow was flexed, these posterior fibers steadily elongated, further decreasing the amount of slack needed to

be overcome before load-bearing could begin. This continued until at 90°, where the posterior fibers were completely taut, and the posterior band had its lowest value of average slack.

5.2 STIFFNESS

5.2.1 Individual Bands

The anterior band had the greatest amount of force per unit of deformation for all three of the represented strain values at 0° and 30° of elbow flexion. This result illustrated the importance of the anterior band in supporting the load within the mUCL at these lower flexion angles.

At 60° of flexion, the anterior band had the second greatest stiffness amongst the three bands at each of the represented strain values. This showed that the role of the other bands towards maintaining stability, in regard to mUCL load-support, started to become comparable to that of the anterior band as the elbow was flexed. This was also shown by the stiffness of the anterior band at 90°, which was the lowest for the band at each strain value.

The middle band had the second greatest stiffness amongst the three bands at 0° and 30° of flexion. This was expected because the anterior band was reported to be the primary stabilizer, in regard to valgus load-support, while the posterior band was reported to provide little toward stability until higher angles of flexion are approached [18]. That the middle band would produce stiffness values between the stiffnesses of these two extremes was reasonable.

At 60° and 90° of elbow flexion, the middle band had the greatest amount of stiffness among the three bands for each of the represented strain values. The anterior band was reported to be the primary stabilizer for valgus loads at these angles [18]. That the middle band displayed

the behavior reported of the anterior band could be a result of the inclusion of some anterior fibers. The large stiffness of the middle band at 60° could be representative of the pending transition of the posterior band as an increased contributor to valgus load support as higher flexion angles were approached.

At 0°, 30° and 60° of elbow flexion, the posterior band had the least amount of stiffness amongst the three for all of the represented strain values. This behavior, in regard to the lesser flexion angles, was in agreement with the reported literature citing the posterior band to contribute little toward valgus load-support at these low angles.

At 90° of flexion, the posterior band had the second greatest stiffness amongst the three bands at two of the represented strain values. When looking at the posterior band alone, a noticeable increase in stiffness could be observed at 90°, in comparison to the previous three angles. This shows that an increase in stiffness and, therefore, an increase in the role of the posterior band in load-support at the elbow does take place as higher angles of flexion were approached.

5.2.2 Overall mUCL

An increase in stiffness was observed from 0° to 30° at each of the prescribed values of strain for the overall mUCL. Because the strain value was held constant, the significant variable was the change in angle. The previous results showed the anterior band to have the second greatest slack and the greatest stiffness at this angle. As the strain increased, the slack became eliminated and the stiffest band, the anterior, became included in the load-bearing. This inclusion resulted in the stiffness increase of the mUCL observed at this angle.

An increase in stiffness was observed from 30° to 60° at each of the prescribed values of strain. This increase could be explained in conjunction with the slack length results. At 60° of elbow flexion, all three bands had relatively similar amounts of slack. This meant that all three bands were able to begin load-support at approximately the same time. With all three bands contributing to load-support sooner, the overall mUCL could support more load per unit of deformation, resulting in a stiffer ligament. This also explained why the stiffness of the ligament was the greatest at this angle.

. From 60° to 90°, the mUCL experienced a decrease in stiffness at each of the represented values of strain. This could be attributed to the shift in the role of the leading band. According to the slack length results, the posterior band had the least slack amongst the three bands at 90°. This meant that the posterior band began to support load sooner than the other two bands at this angle. According to the individual band stiffness results, the posterior band had a low value of stiffness at 90°. The previous leading band, the middle band, had been shown to be much stiffer than the posterior band. Because the least stiff band was beginning to carry load first, it may have deformed significantly and decrease the overall stiffness of the ligament.

5.3 SLACK LENGTH AND STIFFNESS CORRELATION

As discussed in the preceding section, the stiffness results of the overall mUCL can be correlated to the results of the individual band slack lengths. Identifying a correlation between the individual band slack length and the stiffness of the individual bands proved to be more difficult.

On average, the anterior band was the stiffest amongst the three at the flexion angles of 0° and 30°. The slack length results showed the anterior band to have the second most amount of

slack at these two angles. The middle band was the stiffest at 60° and 90°. The slack length for the middle band was lowest at 60° and the second lowest at 90°, in comparison to the other two bands. The posterior band had a low stiffness at 90°, but also had the least amount of slack at this angle.

Investigation of these results does not show an immediate relationship between individual band slack length and individual band stiffness. As noted in the preceding paragraph, the stiffest band may sometimes have the greatest or second greatest amount of slack and the least stiff band may sometimes have the greatest slack. Mechanically speaking, each of these cases has its own respective importance when dealing with the integrity of structures composed of multiple materials. For some structures, the prevention of deformation may be critical and, so, the more deformation-resistant materials are used in areas of the structure that are most likely to see those deformation effects. For other structures, the deformation constraints may be more flexible and the deformation itself may even be encouraged, as in cases where stress alleviation is prioritized.

In relation to the mUCL, utilization of these bands of different stiffness values could be viewed in terms of elbow stability. If the elbow were positioned at an angle where the stability of the motion was most critical, then it would make sense for the stiffest band to have the least slack at that angle. If the stress alleviation at the elbow was instead most critical, it would make sense for the least stiff band to have the least slack at that angle.

The subject of at what point the stability of the elbow motion supersedes the issue of the stress at the elbow, and vice versa, may deal with the influences of the other ligaments at the medial elbow. If the elbow was positioned at an angle where one of the other ligaments assumed most of the motion stability burden, then the mUCL may be relegated to mitigating the stress. In this case, the least stiff band would be more likely to have the least slack. Likewise, if the elbow was

positioned at an angle where one of the other ligaments assumed the majority of the stress alleviation, then the role of the mUCL may transition to that of maintaining motion stability. In this case, the stiffest band would be more likely to have the least slack.

In regard to baseball pitching, the stability and stress concerns at the elbow can be viewed in the way that the forces at the elbow tend to vary in magnitude and direction along the arc of the pitching motion. For positions along the arc where the forces are the most extreme, the elimination of the stresses may be prioritized. For positions where the forces may be less but the angulation may be extreme, maintaining the stability of the motion may take precedence. These kinematic and dynamic variables would have an influence as to which portions of the mUCL and its surrounding counterparts may need to assume which mechanical roles.

The lack of a definitive correlation existing between the slack length and stiffness results of the individual bands do not mean that no such relationship exists. Instead, it suggests that there are other influences that need to be considered and that attempting to identify such a relationship based on analyzing these bands alone may lead to greater difficulties.

This can be reasoned through recognition of the fact that slack length is a geometric property, while stiffness is a material property. A very long steel rope may take longer to begin supporting an imposed load than a shorter aluminum rope. However, once the steel rope reaches full elongation, the essence of its material properties will allow it to support much larger loads than its aluminum counterpart.

There could be some geometric quantities that affect these results as well. As previously noted, the geometric quantities of the ligament are known to vary along the length of the ligament. Geometric variables are independent of slack length and, therefore, a wider or thicker band will be able to support greater loads, irrespective of how much slack it possesses.

The differences in the band stiffness mean that the loads applied to the mUCL will be transmitted differently throughout the bands. The differences in slack length mean that this distribution of loads will also vary as higher loading magnitudes are imposed. Based on the load magnitude, which dictates band elongation, and the band stiffnessess, there could be a preferential transmission of load from one band to the next.

5.4 HYPOTHESIS EVALUATION

The first hypothesis concerned the slack length of each band. It was hypothesized that the anterior band would begin load bearing first at lesser flexion angles and that the posterior band would begin load bearing first at greater flexion angles. At the lower flexion angle of 0°, the middle band had the least amount of slack, which does not support the hypothesis. At the higher flexion angle of 90°, the posterior band had the least amount of slack and the anterior band has the greatest amount, which does supports the hypothesis.

That the anterior band does not have the least slack at the lesser flexion angle could be a consequence of the carry angle. The elbow carry angle, θ, is a natural amount of elbow angulation directed away from the body and has a mean value of $12.88° \pm 5.92°$ [31]. The angle is defined with respect to the central axis of the vertically positioned humerus, as shown in Figure (23).

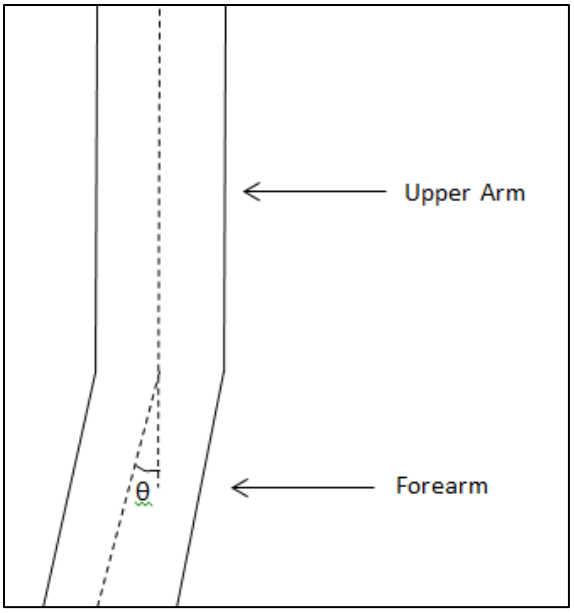

Figure 23. Elbow Carry Angel Representation

This angulation exists in a plane perpendicular to the plane of flexion, but has an effect on the tautness of the mUCL that is proportional to the cosine of the carry angle. This contribution from the carry angle possibly provided an added amount of tension to the ligament. This added tension could have resulted in some additional lengthening of the ligament. The magnitude of this added lengthening would vary between specimens.

The factors that affect the distribution of stresses throughout a body, such as the cross-sectional area, may vary throughout the ligament. Because of this, the added tension from the carry angle could affect different portions of the ligament differently. With regard to the tested specimen, if the middle portion of the ligament possessed some factor less favorable to higher stresses, such as lesser thickness, it would feel a greater effect from the carry angle tension, and elongate more than the other bands. This could explain the middle band having the least amount of slack at the lesser flexion angle.

The second hypothesis concerned the force-strain behavior of each band. It was hypothesized that the anterior band would carry more load at lesser flexion angles, while the load carrying magnitude for the middle and posterior bands would increase with increasing flexion angle. At the lower flexion angles, 0° and 30°, the anterior band was the stiffest of the three bands, on average, which supported the hypothesis. At 60°, the middle band experienced a significant increase in stiffness, and was the stiffest amongst the three bands. At the highest flexion angle, 90°, the posterior band supported more load than it did at the other angles. These results also supported the hypothesis.

The third hypothesis concerned the stiffness of the overall ligament. It was hypothesized that the overall ligament would have the greatest amount of stiffness at either 30° or 60° of elbow flexion. The greatest amount of stiffness was observed to be at 60° of flexion, which supported this hypothesis.

For the posterior and anterior bands, the greatest amount of slack existed at the two extremes of the elbow flexion arc, 0° and 90°, as shown in the slack length results. With the greatest amounts of slack existing at these opposite ends of the flexion arc, it is conceivable that an intermediate value of slack could exist for both at an intermediate flexion angle. This position could possibly be viewed as a position of equilibrium, whereby each band has a relatively equal amount of slack and can begin load-bearing at relatively similar times. This can be seen in the slack length results where all three bands have relatively similar amounts of slack at 60°. With all three bands of the ligament contributing to load support at relatively the same time, the tension can be distributed more evenly throughout the ligament, resulting in less deformation and an overall stiffer ligament.

6.0 CONCLUSION

This study is the first to quantify the mUCL slack length and incorporate it in the construction of the ligament's force-strain response. There is an inherent amount of slack present within the different portions of the mUCL. The amount of slack present in any particular band of the ligament is dependent upon the angle of elbow flexion. At any particular angle, each band possesses a different amount of slack. These findings show that the loading response of the mUCL is dependent upon the sequential loading responses of these different bands following the subsequent elimination of their respective slack.

The anterior and posterior bands behave in a manner consistent with the reported literature in regard to stiffness and laxity. As expected, the lesser flexion angles see a greater influence from the anterior band than the posterior, in regard to stiffness. The higher flexion angles see the role of the anterior band diminish, while that of the middle and posterior bands increase. The inclusion of the middle band produced results for this portion of the ligament that were comparable, and often superior, to those of the anterior and posterior bands. These findings corroborate prior knowledge of the mUCL and show that there may be undocumented portions of the ligament that are just as vital to its performance.

Recognizing that there are several components that make up the mUCL, identifying the behavior of these components and assembling them in a manner which takes into account their inherent laxity, allows for a unique method by which to construct the mechanical force-strain response of the mUCL.

6.1 POSSIBLE IMPLICATIONS

The practical goals of the study were to confirm and quantify certain aspects about the present mUCL knowledge base and to extend it in regard to highlighting the mechanical and geometric behavior of different portions of the ligament. As shown by the presented work, there is a middle portion of the ligament that also possesses distinct mechanical and geometric properties. These characteristics allow this middle band to contribute just as much, if not more, to the overall behavior of the mUCL.

If it can be shown that there are three segments of the ligament which act differently from one another, it could possibly be shown that there are even more. As more experiments are conducted the distinctive nature of each of these segments can be further solidified, and so too could the concept of considering the mUCL as being composed of more than just two distinct segments. This concept solidification could be aided further with the utilization of more advanced technologies such as shear wave elastography. This could result in the advent of new experiments or computer models which aim to incorporate these individualized behaviors when evaluating the performance of the native ligament or newly conceptualized surgical grafts. Future graft models could be of a composite nature, composed of multiple different materials, representing the multiple portions of the mUCL. These materials could all be developed in such a way that their mechanical and geometric properties reflect those of the individual bands of the mUCL.

6.2 LIMITATIONS

Specimen handling, in preparation and testing, may introduce several variables than can affect the output of the experiment. The first variable arises when aligning the markers along the length of the ligament. The alignment of the three rows of markers was used to distinguish the three bands from one another. In the absence of any definitive anatomical landmarks, the placement of these rows was entirely up to the discretion of the operator.

Because of this human element, the portion of the ligament that may be distinguished as one band with one specimen may be different from that same band concerning a different specimen. To mitigate the impact of this variable, each of the rows were equally spaced from one another, regardless of the ligament width. This precaution ensured that the distribution of fibers between each band was approximately equivalent for each specimen. However, it was not possible to keep the fiber distribution constant between specimens.

The testing of the specimen required the successive transection of each ligament band. This operation was performed manually using a surgical scalpel. The initial error arises once more from the discretion of the operator tasked with performing a cut that would maintain the equivalent amount of fibers between the bands. Different amounts of force could have been applied to different regions, which could have resulted in some portions of the bands having larger residual stresses than other portions.

Ideally, each cut was performed directly perpendicular to the ligament surface. This was because any cut performed skew to the surface normal could result in disproportionate band fibers. These compromised fibers could have had a negative effect on the strain output of the bands.

After each transection, the specimen had to be repositioned in the testing apparatus. As the specimen was free to be rotated within the apparatus, it was unlikely that the initial position of

the specimen was able to be exactly replicated during each repositioning. This could have caused some of the markers along the ligament to be in slight miss-focus with the camera system, resulting in lower video quality and possible inaccuracies within the position data.

6.3 FUTURE WORK

Future plans involving the work center around the production of an all-inclusive computer model of the mUCL that can be used to accurately predict the various responses of the ligament to applied disturbances. Many computer models have been made for the mUCL. Most of these involve the use of finite element software. However, these models treat the ligament as a single body, and may not take into account the individual mechanical behavior of the different segments of the ligament.

The results for each band, as reported by the present work, would all be incorporated into the proposed model in order to achieve a more accurate representation of the ligament response. The slack length data would be incorporated so that, under an applied load, the different portions of the band would only begin to strain once their respective slack is eliminated. Once the slack is eliminated, each band would then proceed to strain in a manner consistent with their respective force-strain behavior. At the conclusion of the analysis, the stresses depicted throughout the ligament would be a result of the combined geometric and mechanical effects of each band.

The reliability of the model can be achieved by the continued testing of further specimens. Because the behavioral data for each band utilized by the model will be of an average sense, the more specimens tested will provide greater statistical significance for those average quantities.

The utility of the model can be improved by the inclusion of data taken from the testing of the specimens at more angles.

The realization of such a model would be very useful. Having a reliable tool that can be used to predict the response of the ligament to any given loading scenario, by taking into account the laxity and mechanical behavior of each ligament band, could contribute greatly to athletic, clinical and academic practice.

APPENDIX A

MATLAB CODE

The contents of this appendix include the Matlab code which was used in order to determine the results which are presented in the paper. These include the offset strains (representative of the individual band slack length), the individual band force-strain curves and the force-strain curve of the overall mUCL. This code works in conjunction with the three sets of force-strain data acquired from the tests performed on any particular specimen, as described in the methodology.

```
% function UCL_Superposition
% %Time Synchronization
% %Determining the offset strain values for each band
% %Load strain vs time data for intact ligament
%
% %0 degrees
% % eat0=xlsread('force and strain sheet 8','0','c5:c120');
%anterior
% % emt0=xlsread('force and strain sheet 8','0','b5:b120');          %middle
% % ept0=xlsread('force and strain sheet 8','0','a5:a120');
%posterior
% %30 degrees
% % eat0=xlsread('force and strain sheet 8','30','c5:c100');
%anterior
% % emt0=xlsread('force and strain sheet 8','30','b5:b100');         %middle
% % ept0=xlsread('force and strain sheet 8','30','a5:a100');
%posterior
% %60 degrees
% % eat0=xlsread('force and strain sheet 8','60','c5:c105');
%anterior
% % emt0=xlsread('force and strain sheet 8','60','b5:b105');         %middle
% % ept0=xlsread('force and strain sheet 8','60','a5:a105');
%posterior
% %90 degrees
% % eat0=xlsread('force and strain sheet 8','90','c5:c200');
%anterior
% % emt0=xlsread('force and strain sheet 8','90','b5:b200');         %middle
% % ept0=xlsread('force and strain sheet 8','90','a5:a200');
%posterior
%
%
```

```
% %Removing any negative strain values
% for i=1:length(ept0z)
%     if ept0z(i)>=0
%         ept00(i)=ept0z(i);
%     else
%         ept00(i)=0;
%     end
% end
% for i=1:length(emt0z)
%     if emt0z(i)>=0
%         emt00(i)=emt0z(i);
%     else
%         emt00(i)=0;
%     end
% end
% for i=1:length(eat0z)
%     if eat0z(i)>=0
%         eat00(i)=eat0z(i);
%     else
%         eat00(i)=0;
%     end
% end
%
% %Smoothing the strain data
% sa0=smooth(eat00,1/2);
% sp0=smooth(ept00,1/2);
% sm0=smooth(emt00,1/2);
%
% %Time interval, 0.1s increments
% t=0:0.1:100;
% ta=t(1:length(sa0))';
% tm=t(1:length(sm0))';
% tp=t(1:length(sp0))';
%
% %Differentiating strain w.r.t time
% diffa=max(sa0)-sa0;
% diffm=max(sm0)-sm0;
% diffp=max(sp0)-sp0;
%
% %Finding the index where
% for nna=2:length(diffa)
%         naa(nna)=diffa(nna)/max(sa0);
% end
%
% for nnm=2:length(diffm)
%         nmm(nnm)=diffm(nnm)/max(sm0);
% end
%
% for nnp=2:length(diffp)
%         npp(nnp)=diffp(nnp)/max(sp0);
% end
%
% inda=find(diffa>=0.99*max(naa)*max(sa0),1,'last');
% indm=find(diffm>=0.99*max(nmm)*max(sm0),1,'last');
% indp=find(diffp>=0.99*max(npp)*max(sp0),1,'last');
%
```

```
% %Ordering the indexes of the offset strains from least(band which starts
first) to
% %largest(band which starts last)
% T=[inda indm indp];
% TT=sort(T);
%
% figure(1)
% plot(tp,sp0,'b-')
% hold on
% plot(tm,sm0,'r--')
% hold on
% plot(ta,sa0,'k:')
% hold on
% plot(tp(indp),sp0(indp),'bo','markersize',8)
% hold on
% plot(tm(indm),sm0(indm),'rs','markersize',8)
% hold on
% plot(ta(inda),sa0(inda),'k^','markersize',8)
% legend('Posterior Band','Middle Band','Anterior Band',...
% ['Posterior Band Strain Start Time = ',num2str(tp(indp))],...
% ['Middle Band Strain Start Time = ',num2str(tm(indm))],...
% ['Anterior Band Strain Start Time =
',num2str(ta(inda))],'location','northwest')
% xlabel 'Time (s)'
% ylabel 'Strain (mm/mm)'
% title ('Intact mUCL Strain vs Time ([] Degrees Elbow Flexion)')
%
% %Determining offset strain value
% if TT(1)==indp && TT(2)==indm
%     e_starP=0;
%     e_starM=sp0(indm);
%     e_starA=sp0(inda);
% elseif TT(1)==indp && TT(2)==inda
%     e_starP=0;
%     e_starM=sp0(indm);
%     e_starA=sp0(inda);
% elseif TT(1)==indm && TT(2)==inda
%     e_starP=sm0(indp);
%     e_starM=0;
%     e_starA=sm0(inda);
% elseif TT(1)==indm && TT(2)==indp
%     e_starP=sm0(indp);
%     e_starM=0;
%     e_starA=sm0(inda);
% elseif TT(1)==inda && TT(2)==indm
%     e_starP=sa0(indp);
%     e_starM=sa0(indm);
%     e_starA=0;
% elseif TT(1)==inda && TT(2)==indp
%     e_starP=sa0(indp);
%     e_starM=sa0(indm);
%     e_starA=0;
% end
%
% %%%%%%%%%%%%%%%%%%%%%%%%%%%%%%%%%%%%%%%%%%%%%%%%%%%%%%%%%%%%%%%%%%%%%%%%
% %%%%%%%%%%%%%%%%%%%%%%%%%%%%%%%%%%%%%%%%%%%%%%%%%%%%%%%%%%%%%%%%%%%%%%%%
% %Original exponential-linear code from Dr. Kuxhaus
```

```
% %Used to determine force-strain behavior of posterior band from 2nd
% %transection
%
% global x_p y_p
%
% ep=e_starP;                                   %posterior band strain offset
% em=e_starM;                                   %middle band strain offset
% ea=e_starA;                                   %anterior band strain offset
%
% %Loading the force-strain data for the 2nd transection
%
% %0 degrees
% % ps2=xlsread('force and strain sheet 8','0','ac5:ac50');
% % f2c=xlsread('force and strain sheet 8','0','ad5:ad50');
% % 30 degrees
% % ps2=xlsread('force and strain sheet 8','30','ac5:ac53');
% % f2c=xlsread('force and strain sheet 8','30','ad5:ad53');
% % 60 degrees
% % ps2=xlsread('force and strain sheet 8','60','ac5:ac39');
% % f2c=xlsread('force and strain sheet 8','60','ad5:ad39');
% % 90 degrees
% % ps2=xlsread('force and strain sheet 8','90','ac5:ac158');
% % f2c=xlsread('force and strain sheet 8','90','ad5:ad158');
%
% ps=smooth(ps2,1/2);
% fs=smooth(f2c,1/2);
%
% %%% Select data range to analyze
%     figure(3)
%     plot(ps,fs,'b'); hold on
%     xlabel('Strain (mm/mm)');
%     ylabel('Force (N)');
%     title('Use the mouse to select the end of linear region')
%     [x_lin,~] = ginput(1); % Select the end of linear region
%     ind = find(ps>x_lin,1,'first');
%
%     x_p = ps(1:ind);       % analyzed strain data
%     y_p = fs(1:ind);       % analyzed strain data
%
%     p_max = max(x_p);      % Calculate Data Range
%
% %%% Optimize the cost function (square error)
%
%     % Intial Parameters for Model Optimization
%     a = 0.25;                    % exponential function scaling parameter
(.25)
%     b = 50;                   % exponent (50)
%     p = 0.05;                    % x-location of the transition point
(p,q) (.05)
%
%     vi = [a,b,p];             % Put input variables into matrix form
%     lb = [0,0,0];             % Set the lower bounds
%     ub = [1000,5000,p_max];   % Set the upper bounds
%
%     % Finds optimized variable values to minimize the cost function
%     options = optimset('Display','iter','MaxFunEvals',1000);
%     vo = fmincon(@posterior,vi,[],[],[],[],lb,ub,[],options);
```

```
%
% %%% Calculate the Curves and the Error
%     a = vo(1);              % reassign variables
%     b = vo(2);
%     p = vo(3);
%     q = a*(exp(b*p)-1);    % y value at (p,q)
%     c = a*b*exp(b*p);      % dy/dx value at (p,q) & slope of linear
function
%     W=0;                   % initialize the weighting function
%
%      for i = 1:length(x_p)
%         if (x_p(i)<p)
%             y(i) = a*(exp(b*x_p(i))-1);   % Toe section of the stress curve
%         else
%             y(i) = c*(x_p(i)-p) + q;      % Linear section of the stress
curve
%         end
%         w2(i)= (y_p(i)- y(i))^2;          % Calculate the square of the
error
%         W = W + w2(i);                    % Calculate the sum of the square
error
%      end
%
% %%% Plot Stress-Strain Curve
%     figure(4)
%     plot(ps,fs,'c.',x_p, y_p,'.b')
%     hold on
%     plot(x_p,y,'om-','MarkerSize',3)
%     hold on
%     plot(p,q,'pm','MarkerSize',12)
%     hold on
%     plot(x_p,w2,'r-', 'MarkerSize',1)
%     xlabel('Strain (mm/mm)')
%     ylabel('Force (N)')
%     title ('Force vs Strain Posterior Band ([] degrees,2nd Transection)')
%     legend('Measured','Analyzed','Modeled','Transition
Point','MSE','Location','northwest')
%     set(gcf,'PaperPositionMode','manual')
%
%    UCL_SuperpositionF1(a,b,c,p,q,ep,em,ea)
%  end
% %%%%%%%%%%%%%%%%%%%%%%%%%%%%%%%%%%%%%%%%%%%%%%%%%%%%%%%%%%%%%%%%%%%%%%%%%%%
% %Minimizing the difference between the measured and modeled posterior band
% %forces
%
%     function [W] = posterior(vi)
%
% global x_p y_p
%
%  a = vi(1);                              % Re-assign variables
%  b = vi(2);
%  p = vi(3);
%  q = a*(exp(b*p)-1);                     % y value at (p,q)
%  c = a*b*exp(b*p);                       % dy/dx value at (p,q) & slope of
linear function
%  W=0;                                    % initialize the weighting function
%
```

```
%     for ii = 1:length(x_p)
%         if (x_p(ii)<p)
%             y(ii) = a*(exp(b*x_p(ii)-1));   % Toe section of the stress
curve
%         else
%             y(ii) = c*(x_p(ii)-p) + q;      % Linear section of the stress
curve
%         end
%         w2(ii)= (y_p(ii)- y(ii))^2;         % Calculate the square of the
error
%         W = W + w2(ii);                     % Calculate the sum of the
square error
%     end
%     end
%
% %%%%%%%%%%%%%%%%%%%%%%%%%%%%%%%%%%%%%%%%%%%%%%%%%%%%%%%%%%%%%%%%%%%%%%%
% %Determining the middle band force-strain behavior
%
% function UCL_SuperpositionF1(a,b,c,p,q,ep,em,ea)
%
% global ffm1c ms1
%
% %Loading the force-strain data for middle and posterior bands for 1st
% %transection
%
% %0 degrees
% % ps1=xlsread('force and strain sheet 8','0','y5:y33');
% % ms1=xlsread('force and strain sheet 8','0','z5:z33');
% % f1c=xlsread('force and strain sheet 8','0','aa5:aa33');
% %30 degrees
% % ps1=xlsread('force and strain sheet 8','30','y5:y46');
% % ms1=xlsread('force and strain sheet 8','30','z5:z46');
% % f1c=xlsread('force and strain sheet 8','30','aa5:aa46');
% %60 degrees
% % ps1=xlsread('force and strain sheet 8','60','y5:y20');
% % ms1=xlsread('force and strain sheet 8','60','z5:z20');
% % f1c=xlsread('force and strain sheet 8','60','aa5:aa20');
% %90 degrees
% % ps1=xlsread('force and strain sheet 8','90','y5:y137');
% % ms1=xlsread('force and strain sheet 8','90','z5:z137');
% % f1c=xlsread('force and strain sheet 8','90','aa5:aa137');
%
% %Ordering the strains and keeping correct force-strain pairs w.r.t time
% A1=[ps1 f1c];
% [~,sorted_inds]=sort(A1(:,1));
% B1=A1(sorted_inds,:);
%
% %Calculating posterior band forces
% for jj=1:length(B1(:,1))
%     if B1(jj)<=p
%             pf1c(jj)= a*(exp(b*B1(jj,1))-1);
%     else
%             pf1c(jj)=c*(B1(jj,1)-p) + q;
%     end
% end
%
% %Imposing that the middle band forces be equal to the difference between
```

```
% %the total measured force and the posterior forces
% midf=B1(:,2)-pf1c';
%
% %removing any negative values
% for x=1:length(midf)
%     if midf(x)>=0
%        midf1c(x)=midf(x);
%     else
%         midf1c(x)=0;
%     end
% end
%
% h=find(midf1c);
% fm1c=[0,midf1c(h)];
% ffm1c=sort(fm1c);
% fm_max = max(ffm1c);
%
%
% %Determining the middle band model parameters
%
% am=0.25;
% bm=50;
% qm=0.05;
%
% v = [am,bm,qm];                % Put input variables into matrix form
% lb = [0,0,0];                  % Set the lower bounds
% ub = [1000,1000,fm_max];       % Set the upper bounds
%
%  % Finds optimized variable values to minimize the cost function
%   wo = fmincon(@middle,v,[],[],[],[],lb,ub);
%   %%% Calculate the Curves
%   am = wo(1);                                % reassign variables
%   bm = wo(2);
%   qm = wo(3);
%   pm=(log((qm/am)+1))/bm;                    % strain value at (pm,qm)
%   cm = am*bm*exp(bm*pm);                     % dy/dx value at (pm,qm) & slope
of linear function
%   W1=0;                                      % initialize the weighting
function
%
%   for xx = 1:length(ffm1c)
%         if (ffm1c(xx)<=qm)
%             em1c(xx) = (log((ffm1c(xx)/am)+1))/bm;   % Toe section of the
stress curve
%         else
%             em1c(xx) = ((ffm1c(xx)-qm)/cm)+pm;       % Linear section of
the stress curve
%         end
%         w2(xx)= (ms1(xx)-em1c(xx))^2;                % Calculate the square
of the error
%         W1 = W1 + w2(xx);                            % Calculate the sum of
the square error
%   end
%
%
% UCL_SuperpositionF2(a,b,c,p,q,am,bm,cm,pm,qm,ea,em,ep)
% end
```

```
%
% %%%%%%%%%%%%%%%%%%%%%%%%%%%%%%%%%%%%%%%%%%%%%%%%%%%%%%%%%%%%%%%%%%%%%%%%%%
% %Minimizing the difference between the measured and modeld middle band
strain data
%
% function [W1] = middle(v)
%
% global ffm1c ms1
%
% am = v(1);                                        % Re-assign variables
% bm = v(2);
% qm = v(3);
% pm=(log((qm/am)+1))/bm;                           % y value at (p,q)
% cm = am*bm*exp(bm*pm);                            % dy/dx value at (p,q) &
slope of linear function
% W1=0;                                             % initialize the
weighting function
%
%     for xi = 1:length(ffm1c)
%         if (ffm1c(xi)<=qm)
%             em1c(xi) = (log((ffm1c(xi)/am)+1))/bm;   % Toe section of the
stress curve
%         else
%              em1c(xi) = ((ffm1c(xi)-qm)/cm)+pm;      % Linear section of
the stress curve
%         end
%         w2(xi)= (ms1(xi)-em1c(xi))^2;                % Calculate the square
of the error
%         W1 = W1 + w2(xi);                            % Calculate the sum of
the square error
%     end
% end
%
% %%%%%%%%%%%%%%%%%%%%%%%%%%%%%%%%%%%%%%%%%%%%%%%%%%%%%%%%%%%%%%%%%%%
% %Determining the anterior band force-strain behavior
%
% function UCL_SuperpositionF2(a,b,c,p,q,am,bm,cm,pm,qm,ea,em,ep)
% global ffant as0
% %Loading the force-strain data for the anterior, middle, and posterior
bands
% %for the intact ligament
%
% %0 degrees
% % ps0=xlsread('force and strain sheet 8','0','t5:t47');
% % ms0=xlsread('force and strain sheet 8','0','u5:u47');
% % as0=xlsread('force and strain sheet 8','0','v5:v47');
% % f0c=xlsread('force and strain sheet 8','0','w5:w47');
% %30 degrees
% % ps0=xlsread('force and strain sheet 8','30','t5:t41');
% % ms0=xlsread('force and strain sheet 8','30','u5:u41');
% % as0=xlsread('force and strain sheet 8','30','v5:v41');
% % f0c=xlsread('force and strain sheet 8','30','w5:w41');
% %60 degrees
% % ps0=xlsread('force and strain sheet 8','60','t5:t30');
% % ms0=xlsread('force and strain sheet 8','60','u5:u30');
% % as0=xlsread('force and strain sheet 8','60','v5:v30');
% % f0c=xlsread('force and strain sheet 8','60','w5:w30');
```

```
% %90 degrees
% % ps0=xlsread('force and strain sheet 8','90','t5:t131');
% % ms0=xlsread('force and strain sheet 8','90','u5:u131');
% % as0=xlsread('force and strain sheet 8','90','v5:v131');
% % f0c=xlsread('force and strain sheet 8','90','w5:w131');
%
%
% %Time indexes
% time=1:length(ps0);
%
% %Ordering the strains and keeping correct force-strain pairs w.r.t time
% C=[ps0 ms0 f0c time'];
% [~,sorted_inds]=sort(C(:,1));                  %sorting posterior strains
% [~,sorted_inds2]=sort(C(:,2));                 %sorting middle strains
% D=C(sorted_inds,:);
% E=C(sorted_inds2,:);
% I=[D(:,4) E(:,4)];
%
% %Calculating posterior forces
% for ji=1:length(D(:,1))
%     if D(ji,1)<=p
%            pf0c(ji)=a*(exp(b*D(ji,1))-1);
%     else
%            pf0c(ji)=c*(D(ji,1)-p) + q;
%     end
% end
%
% %Calculating middle band forces
% for r=1:length(E(:,2))
%     if E(r,2)<=pm
%            mf0c(r) = am*(exp(bm*E(r,2))-1);
%     else
%            mf0c(r)=cm*(E(r,2)-pm) + qm;
%     end
% end
%
% %Matching forces with correct indices
% %Superposing the anterior forces as the difference between the total
% %meaured force and the sum of the middle and posterior forces
% for rr=time
%     for er=time
%         if I(rr,1)==I(er,2)
%             sum(rr)=pf0c(rr)+mf0c(er);
%             antf(rr,1)=f0c(I(rr,1))-sum(rr);
%         end
%     end
% end
%
% %Removing any negative force values
% for iij=1:length(antf)
%     if antf(iij)>=0
%         antff(iij)=antf(iij);
%     elseif antf(iij)<0
%         antff(iij)=0;
%     end
% end
%
```

```
% cc=find(antff);
% fant=[0,antff(cc)];
% ffant=sort(fant);
% fa_max = max(ffant);
%
% %Determining the anterior band model parameters
% aa=0.25;
% ba=50;
% qa=0.05;
%
% vii = [aa,ba,qa];               % Put input variables into matrix form
% lb = [0,0,0];                   % Set the lower bounds
% ub = [1000,5000,fa_max];        % Set the upper bounds
%
% % Finds optimized variable values to minimize the cost function
%
%   voo = fmincon(@anterior,vii,[],[],[],[],lb,ub);
%   %%% Calculate the Curves
%   aa = voo(1);                                    % reassign variables
%   ba = voo(2);
%   qa = voo(3);
%   pa=(log((qa/aa)+1))/ba;                         % strain value at (pm,qm)
%   ca = aa*ba*exp(ba*pa);                          % dy/dx value at (pm,qm) &
slope of linear function
%   W2=0;                                           % initialize the weighting
function
%    for ai = 1:length(ffant)
%         if (ffant(ai)<qa)
%             ea0(ai) = log((ffant(ai)/aa)+1)/ba;  % Toe section of the
stress curve
%         else
%             ea0(ai) = (ffant(ai)-qa)/ca+pa;      % Linear section of the
stress curve
%         end
%         w2(ai)= (as0(ai)-ea0(ai))^2;            % Calculate the square of
the error
%         W2 = W2 + w2(ai);                       % Calculate the sum of the
square error
%    end
%
%
% %Smoothing the curves by evaluation at very fine strain intervals
% %Arbitray strain interval
% ee=0:0.0000001:0.1;
% eL=length(ee);
%
% for gj=1:length(ee)                                 %posterior
%     if ee(gj)<=p
%         fp(gj)= a*(exp(b*ee(gj))-1);
%     else
%         fp(gj)=c*(ee(gj)-p) + q;
%     end
% end
%
%
% for gi=1:length(ee)                                 %middle
%     if ee(gi)<=pm
```

```
%        fm(gi)=am*(exp(bm*ee(gi))-1);
%     else
%         fm(gi)=cm*(ee(gi)-pm) + qm;
%     end
% end
%
%
% for gd=1:length(ee)                                    %anterior
%     if ee(gd)<=pa
%         fa(gd)=aa*(exp(ba*ee(gd))-1);
%     else
%         fa(gd)=ca*(ee(gd)-pa) + qa;
%     end
% end
%
% %%%%%%%%%%%%%%%%%%%%%%%%%%%%%%%%%%%%%%%%%%%%%%%%%%%%%%%%%%%%%%%%%%%%%%%%
% %Calculating the sequential force sum
% %Finding order of offset strain values
% Ez=[ea ep em];
% EE=sort(Ez);
%
% %Finding the index of the offset strain values within the strain range ee
% na=find(ee>=0.99*ea,1,'first');
% nm=find(ee>=0.99*em,1,'first');
% np=find(ee>=0.99*ep,1,'first');
%
% %Calculating strain intervals
% if EE(1)==ep
%     epp=ee;
%     emm(1:nm)=zeros(1,nm);
%     emm(nm+1:eL)=ee(1:eL-nm);
%     eaa(1:na)=zeros(1,na);
%     eaa(na+1:eL)=ee(1:eL-na);
% elseif EE(1)==em
%     emm=ee;
%     epp(1:np)=zeros(1,np);
%     epp(np+1:eL)=ee(1:eL-np);
%     eaa(1:na)=zeros(1,na);
%     eaa(na+1:eL)=ee(1:eL-na);
% elseif EE(1)==ea
%     eaa=ee;
%     epp(1:np)=zeros(1,np);
%     epp(np+1:eL)=ee(1:eL-np);
%     emm(1:nm)=zeros(1,nm);
%     emm(nm+1:eL)=ee(1:eL-nm);
% end
%
% %Evaluating the forces for each band within strain interval
% for jjj=1:length(epp)                                  %posterior
%     if epp(jjj)<=p
%        fpp(jjj)= a*(exp(b*epp(jjj))-1);
%     else
%        fpp(jjj)=c*(epp(jjj)-p) + q;
%     end
% end
%
% for iii=1:length(emm)                                  %middle
```

```
%     if emm(iii)<=pm
%        fmm(iii)=am*(exp(bm*emm(iii))-1);
%     else
%        fmm(iii)=cm*(emm(iii)-pm) + qm;
%     end
% end
%
% for ddd=1:length(eaa)                                    %anterior
%     if eaa(ddd)<=pa
%        faa(ddd)=aa*(exp(ba*eaa(ddd))-1);
%     else
%        faa(ddd)=ca*(eaa(ddd)-pa) + qa;
%     end
% end
%
% %Summing up the forces in each band
% UCLforce=fpp(1:end)+fmm(1:end)+faa(1:end);
% %%%%%%%%%%%%%%%%%%%%%%%%%%%%%%%%%%%%%%%%%%%%%%%%%%%%%%%%%%%%%%%%%%%%%%%%
% %Plotting individual posterior,middle, & anterior force-strain curves
% fend=find(UCLforce>=0.99*max(f0c),1,'first');
%
% figure(5)
% plot(epp,fpp,'b-')
% hold on
% plot(emm,fmm,'r--')
% hold on
% plot(eaa,faa,'k:')
% axis([0 ee(fend) 0 max(f0c)])
% title('Individual Band Force vs Strain ([] degrees)')
% legend('Posterior','Middle','Anterior','location','northwest')
% xlabel 'Strain (mm/mm)'
% ylabel 'Force (N)'
%
%
UCL_final(UCLforce,a,b,c,p,q,am,bm,cm,pm,qm,ea,em,ep,aa,ba,ca,pa,qa,fend,ee,n
p,nm,na,epp,emm,eaa,fpp,fmm,faa,f0c)
% end
% %%%%%%%%%%%%%%%%%%%%%%%%%%%%%%%%%%%%%%%%%%%%%%%%%%%%%%%%%%%%%%%%%%%%%%%%
% %Minimizing the difference between the measured and modeld anterior band
strain data
%
% function [W2] = anterior(vii)
%
% global ffant as0
%
% aa = vii(1);                                        % Re-assign variables
% ba = vii(2);
% qa = vii(3);
% pa=(log((qa/aa)+1))/ba;                             % y value at (p,q)
% ca = aa*ba*exp(ba*pa);                              % dy/dx value at (p,q) &
slope of linear function
% W2=0;                                               % initialize the
weighting function
%
%     for i = 1:length(ffant)
%         if (ffant(i)<qa)
```

```
%             ea0(i) = log((ffant(i)/aa)+1)/ba;   % Toe section of the stress
curve
%         else
%              ea0(i) = (ffant(i)-qa)/ca+pa;      % Linear section of the
stress curve
%         end
%         w2(i)= (as0(i)-ea0(i))^2;               % Calculate the square of
the error
%         W2 = W2 + w2(i);                        % Calculate the sum of the
square error
%     end
% end
%
% %%%%%%%%%%%%%%%%%%%%%%%%%%%%%%%%%%%%%%%%%%%%%%%%%%%%%%%%%%%%%%%%%%%%%%%%%%%
% %Calculating the force-strain behavior for the total mUCL
%
% function
UCL_final(UCLforce,a,b,c,p,q,am,bm,cm,pm,qm,ea,em,ep,aa,ba,ca,pa,qa,fend,ee,n
p,nm,na,epp,emm,eaa,fpp,fmm,faa,f0c)
% global x_p1 y_p1
%
% x_p1=ee(1:10000:fend);
% y_p1=UCLforce(1:10000:fend);
%
% p_maxf = max(x_p1);            % Calculate Data Range
%
% au=0.25;
% bu=50;
% pu=0.05;
%
% viii = [au,bu,pu];              % Put input variables into matrix form
% lb = [0,0,0];                   % Set the lower bounds
% ub = [1000,5000,p_maxf];        % Set the upper bounds
%
% %Finds optimized variable values to minimize the cost function
%
%   vooo = fmincon(@UCL,viii,[],[],[],[],lb,ub);
%   %%% Calculate the Curves
%   au = vooo(1);                   % reassign variables
%   bu = vooo(2);
%   pu = vooo(3);
%   qu = au*(exp(bu*pu)-1);       % y value at (p,q)
%   cu = au*bu*exp(bu*pu);        % dy/dx value at (p,q) & slope of linear
function
%   W3=0;                         % initialize the weighting function
%      for ui = 1:length(x_p1)
%         if (x_p1(ui)<=pu)
%             yf(ui) = au*(exp(bu*x_p1(ui))-1);   % Toe section of the stress
curve
%         else
%             yf(ui) = cu*(x_p1(ui)-pu) + qu;      % Linear section of the
stress curve
%         end
%         w3(ui)= (y_p1(ui)- yf(ui))^2;          % Calculate the square of
the error
%         W3 = W3 + w3(ui);                    % Calculate the sum of the
square error
```

```
%      end
% %%%%%%%%%%%%%%%%%%%%%%%%%%%%%%%%%%%%%%%%%%%%%%%%%%%%%%%%%%%%
% for xf = 1:length(ee)
%         if (ee(xf)<=pu)
%             yff(xf) = au*(exp(bu*ee(xf))-1);
%         else
%             yff(xf) = cu*(ee(xf)-pu) + qu;
%         end
% end
%
% ffendd=find(yff>=0.99*max(f0c),1,'first');
% %%%%%%%%%%%%%%%%%%%%%%%%%%%%%%%%%%%%%%%%%%%%%%%%%%%%%%%%%%%%
% %Plotting Stress-Strain Curves
% figure(7)
% plot(ee,UCLforce,'k-','markersize',8)
% hold on
% plot(ee(np),UCLforce(np),'ko','markersize',8)
% hold on
% plot(ee(nm),UCLforce(nm),'ks','markersize',8)
% hold on
% plot(ee(na),UCLforce(na),'k^','markersize',8)
% axis([0 ee(fend) 0 UCLforce(fend)])
% xlabel 'Strain (mm/mm)'
% ylabel 'Force (N)'
% legend('UCL Force  (Leading Band Strain,Force)',...
%   ['Posterior Band = (',num2str(ep),',',num2str(UCLforce(np)),')'],...
%   ['Middle Band = (',num2str(em),',',num2str(UCLforce(nm)),')'],...
%   ['Anterior Band =
(',num2str(ea),',',num2str(UCLforce(na)),')'],'location','northwest')
% title ('mUCL Force vs Strain [] degrees')
%
% figure(8)
% plot(x_p1,y_p1,'b.')
% hold on
% plot(x_p1,yf,'om-','MarkerSize',3)
% hold on
% plot(pu,qu,'pm','MarkerSize',12)
% hold on
% plot(x_p1,w3,'r-', 'MarkerSize',1)
% axis([0 x_p1(end) 0 y_p1(end)])
% xlabel('Strain (mm/mm)')
% ylabel('Force (N)')
% title ('mUCL Force vs Strain [] degrees-Curve Fit')
% legend('Analyzed','Modeled','Transition
Point','MSE','Location','northwest')
% set(gcf,'PaperPositionMode','manual')
%
% figure(9)
% plot(ee,yff,'k','MarkerSize',3)
% axis([0 ee(ffendd) 0 yff(ffendd)])
% xlabel('Strain (mm/mm)')
% ylabel('Force (N)')
% title ('mUCL Force vs Strain [] degrees')
%
% figure(10)
% plot(ee,yff,'k','MarkerSize',3)
% hold on
```

```
% plot(ee(np),yff(np),'ko','markersize',8)
% hold on
% plot(ee(nm),yff(nm),'ks','markersize',8)
% hold on
% plot(ee(na),yff(na),'k^','markersize',8)
% axis([0 ee(ffendd) 0 yff(ffendd)])
% xlabel('Strain (mm/mm)')
% ylabel('Force (N)')
% legend('mUCL Force','Posterior','Middle','Anterior','location','northwest')
% title ('mUCL Force vs Strain [] degrees')
%
% %Storing and printing the model parameters for each band
%
% P=[a b c p q];
% M=[am bm cm pm qm];
% A=[aa ba ca pa qa];
% U=[au bu cu pu qu];
% D=[A; M; P; U]';
%
% fileID=fopen('Parameters_90degrees_T8.txt','w');
% fprintf(fileID,'%1$s\r\n','Parameters for Stress-Strain Exponential
Model');
% fprintf(fileID,'%1$s %2$s %3$s %4$s\r\n','Row 1-Anterior Band','Row 2-
Middle Band','Row 3-Posterior Band','Row 4-Total');
% fprintf(fileID,'%1$s %2$s %3$s %4$s %5$s\r\n','a','      b','      c','
p','      q');
% fprintf(fileID,'%6.4f %6.4f %6.4f %6.4f %6.4f\r\n',D);
%
% end
% %%%%%%%%%%%%%%%%%%%%%%%%%%%%%%%%%%%%%%%%%%%%%%%%%%%%%%%%%%%%%%%%%%%%%%%%%%%%
%
% function [W3] = UCL(viii)
%
% global x_p1 y_p1
%
%  au = viii(1);                          % Re-assign variables
%  bu = viii(2);
%  pu = viii(3);
%  qu = au*(exp(bu*pu)-1);                % y value at (p,q)
%  cu = au*bu*exp(bu*pu);                 % dy/dx value at (p,q) & slope of
linear function
%  W3=0;                                  % initialize the weighting
function
%
%     for uii = 1:length(x_p1)
%         if (x_p1(uii)<=pu)
%             yf(uii) = au*(exp(bu*x_p1(uii)-1));    % Toe section of the
stress curve
%         else
%             yf(uii) = cu*(x_p1(uii)-pu) + qu;      % Linear section of the
stress curve
%         end
%         w3(uii)= (y_p1(uii)- yf(uii))^2;           % Calculate the square
of the error
%         W3 = W3 + w3(uii);
%     end
% end
```

BIBLIOGRAPHY

1. Reagan WD, Korinek SL, Morrey BF, An K, *Biomechancial Study of Ligaments Around the Elbow Joint.* Clin Orthop, 1991. **271**: p. 170-179.

2. Fuss FK, *The ulnar collateral ligament of the human elbow joint. Anatomy, function, and biomechanics.* J Anat, 1990. **175**: p. 203-212.

3. Lee TQ, Gupta R, Fornalski S, *Anatomy and Biomechanics of the Elbow Joint.* Sports Med Arthrosc Rev, 2003. **7**(4): p. 168-178.

4. Timmerman LA, Andrews JR, *Histology and Arthroscopic Anatomy of the Ulnar Collateral Ligament of the Elbow.* Sports Medicine, 1994. **22**(5): p. 667-673.

5. Ciccotti MG, Atanda Jr A, Nazarian LN, Dodson CC, Holmes L, Cohen SB, *Stress Sonography of the Ulnar Collateral Ligament of the Elbow in Professional Baseball Pitchers.* Am J Sports Med, 2014. **42**(3): p. 544-551.

6. Dugas JR, Ostrander RV, Cain EL, Kingsley D, Andrews JR, *Anatomy of the anterior bundle of the ulnar collateral ligament.* J Shoulder Elbow Surg, 2007. **16**(5): p. 657-660.

7. Farrow LD, Mahoney AJ, Stefancin JJ,Taljanovic MS,Sheppard JE,Schickendantz MS, *Quantitative Analysis of the Medial Ulnar Collateral Ligament Ulnar Footprint and Its Relationship to the Ulnar Sublime Tubercle.* Am J Sports Med, 2011. **39**(9): p. 1936-1941.

8. Hibberd EE, Brown JR, Hoffer JT, *Optimal management of ulnar collateral ligament injury in baseball pitchers.* Open Access J Sports Med, 2015. **6**: p. 343-352.

9. Anz AW, Bushnell BD, Griffin LP, Noonan TJ, Torry MR, Hawkins RJ, *Correlation of Torque and Elbow Injury in Professional Baseball Pitchers.* Am J Sports Med, 2010. **38**(7): p. 1368-1374.

10. Bushnell BD, Anz AW, Noonan TJ, Torry MR, Hawkins RJ, *Association of Maximum Pitch Velocity and Elbow Injury in Professional Baseball Pitchers.* Am J Sports Med, 2010. **38**(4): p. 728-732.

11. Werner SL, Fleisig GS, Dillman CJ, Andrews JR, *Biomechanics of the Elbow druing Baseball Pitching.* J Orthop Sports Phys Ther, 1993. **17**(6): p. 274-278.

12. Fleisig GS, Escamilla RF, *Kinetics of Baseball Pitching with Implications About Injury Mechanics.* Am J Sports Med, 1995. **23**(2): p. 233-239.

13. Aguinaldo AL, Chambers H, *Correlation of Throwing Mechanics With Elbow Valgus Load in Adult Baseball Pitchers.* Am J Sports Med, 2009. **37**(10): p. 2043-2048.

14. Beckett KS, McConnell P, Lagopoulos M, Newman RJ, *Variations in the normal anatomy of the collateral ligaments of the human elbow joint.* J Anat, 2000. **197**: p. 507-511.

15. Morrey BF, AN Kai-Nan, *Articular and ligamentous contributions to the stability of the elbow joint.* Am J Sports Med, 1983. **11**(5): p. 315-319.

16. Eygendaal D, Olsen BS, Jensen SL, Seki A, Sojbjerg JO, *Kinematics of partial and total ruptures of the medial collateral ligament of the elbow.* J Shoulder Elbow Surg, 1999. **8**(6): p. 612-616.

17. Jackson, T. J., Jarrell, S. E., Adamson, G. J., Chung, K. C., Lee, T. Q., *Biomechanical Differences of the Anterior and Posterior Bands of the Ulnar Collateral Ligament of the Elbow.* Knee Surg Sports Traumatol Arthrosc, 2016. **24**(7): p. 2319-23.

18. Floris S, Olsen BO, Dalstra M, Sojbjerg JO, Sneppen O, *The medial collateral ligament of the elbow joint: Anatomy and Kinematics.* J Shoulder Elbow Surg, 1998. **7**(4): p. 345-351.

19. Buffi JH, Werner K, Kepple T, Murray WM, *Computing Muscle, Ligament, and Osseous Contributions to the Elbow Varus Moment During Baseball Pitching.* Ann Biomed Eng, 2015. **43**(2): p. 404-415.

20. Cain EL Jr, Dugas JR, Andrews JR, *Elbow Injuries in Throwing Athletes: A Current Concepts Review.* Am J Sports Med, 2003. **31**(4): p. 621-635.

21. Wilson AT, Pidgeon T, Dasilva MF, Morrelll N, *Trends in Elbow Ulnar Collateral Ligament Reconstruction in Professional Baseball Pitchers.* J Hand Surg 2015. **40**(9): p. 23-24.

22. Erickson BJ, Harris JD, Chalmers PN, Bach Jr BR, Verma NN, Bush-Joseph CA, Romeo AA, *Ulnar Collateral Liagment Reconstruction: Anatomy, Indications, Techniques, and Outcomes.* Sports Health, 2015. **7**(6): p. 511-517.

23. Dodson CC, Thomas A, Dines JS, Nho SJ, Williams II RJ, Altchek DW, *Medial Ulnar Collateral Ligament Reconstruction of the Elbow in Throwing Athletes.* Am J Sports Med, 2006. **34**(12): p. 1926-1932.

24. Ruland RT, Hogan CJ, Randall CJ, Richards A, Belkoff SM, *Biomechanical Comparison of Ulnar Collateral Ligament Reconstruction Techniques.* Am J Sports Med, 2008. **36**(8): p. 1565-1570.

25. Paletta Jr GA, Klepps SJ, Difelice GS, Allen T, Brodt MD, Burns ME, Silva MJ, Wright RW, *Biomechanical Evaluation of two Techniques for Ulnar Collateral Ligament Reconstruction of the Elbow.* Am J Sports Med, 2006. **34**(10): p. 1599-1603.

26. Ciccotti MG, Siegler S, Kuri II JA, Thinnes JH, Murphy IV DJ, *Comparison of the Biomechanical Profile of the Intact Ulnar Collateral Ligament With the Modified Jobe and the Docking Reconstructed Elbow.* Am J Sports Med, 2009. **37**(5): p. 974-981.

27. Cain Jr. EL, Andrews JR, Dugas JR, Wilk KE, McMichael CS, Walter II JC, Riley RS, Arthur ST, *Outcome of Ulnar Collateral Ligament Reconstruction in 1281 Athletes.* Am J Sports Med, 2010. **38**(12): p. 2426-2434.

28. Wilson AT, Pidgeon TS, Morrell NT, DaSilva MF, *Trends in Revision Elbow Ulnar Collateral Ligament Reconstruction in Professional Baseball Pitchers.* J Hand Surg Am, 2015. **40**(11): p. 2249-2254.

29. Fung YC, *"Elasticity of Soft Tissues in Simple Elongation".* Am J Physiol, 1967. **213**(6): p. 1532-1544.

30. Kuxhaus L, Miller MC, Weisenbach CA, Tanaka ML, *A Continous Mehod to Compute Model Parameters for Soft Biological Materials.* J Biomech Eng, 2011. **133**(7): p. 074502.

31. Paraskevas G, Papadopoulos A, Papaziogas B, Spanidou S, Argiriadou H, Gigis J, *Study of the Carrying Angle of the Human Elbow Joint in Full Extension: A Morphometric Analysis.* Surg Radiol Anat, 2004. **26**(1): p. 19-23.